AD-A044 993 CONSTRUCTION ENGINEERING RESEARCH LAB (ARMY) CHAMPAI--ETC F/G 20/4
LIQUID-SPRING SHOCK ISOLATOR MODELING.(U)
SEP 77 P N SONNENBURG, B H WENDLER

UNCLASSIFIED CERL-TR-M-226 NL

| OF |
AD
A044 993

END
DATE
FILMED
11-77
DDC

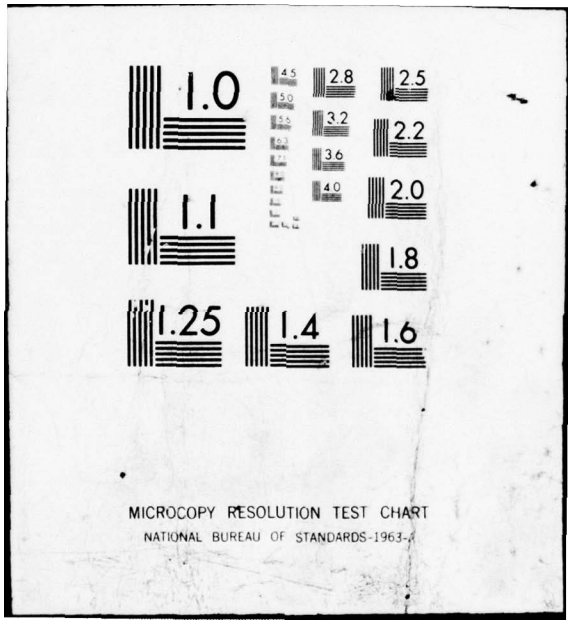
1.0
1.1
1.25
1.4
1.6
1.8
2.0
2.2
2.5
2.8
3.2
3.6
4.0
4.5
5.0
MICROCOPY RESOLUTION TEST CHART
NATIONAL BUREAU OF STANDARDS-1963-A

construction
engineering
research
laboratory

TECHNICAL REPORT M-226
September 1977

LIQUID-SPRING SHOCK ISOLATOR MODELING

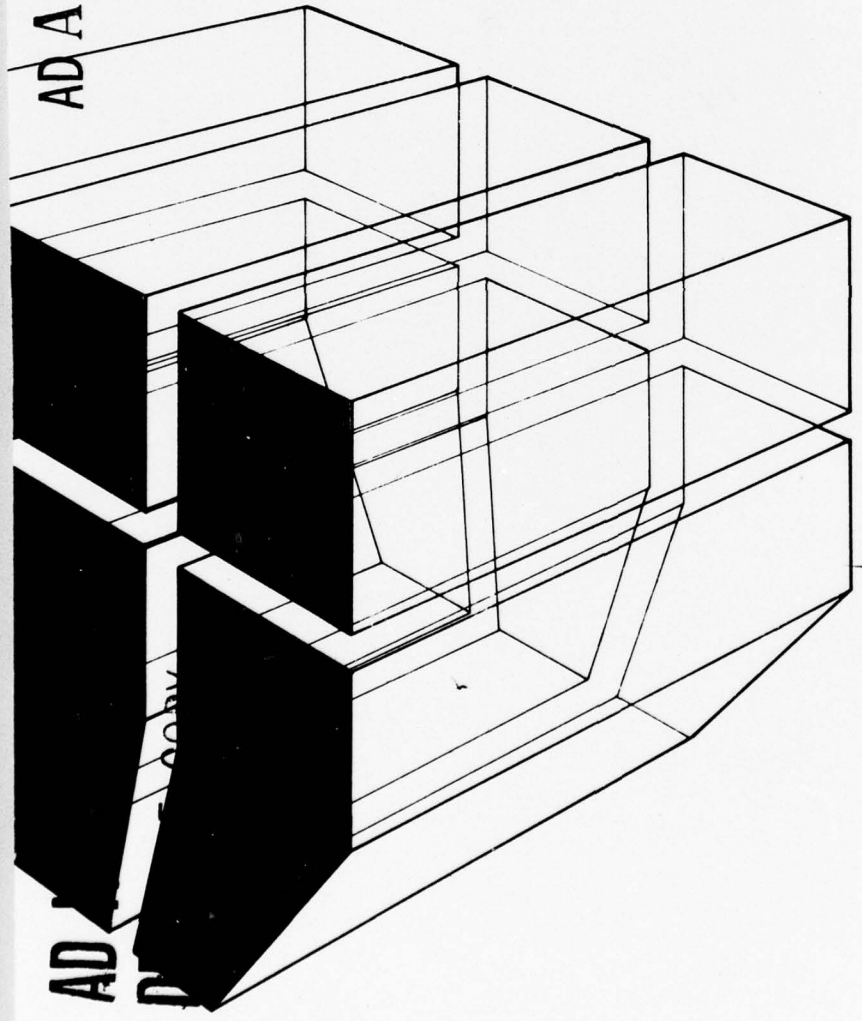

by
P. N. Sonnenburg
B. H. Wendler
W. E. Fisher

CERL

The contents of this report are not to be used for advertising, publication, or promotional purposes. Citation of trade names does not constitute an official indorsement or approval of the use of such commercial products. The findings of this report are not to be construed as an official Department of the Army position, unless so designated by other authorized documents.

DESTROY THIS REPORT WHEN IT IS NO LONGER NEEDED
DO NOT RETURN IT TO THE ORIGINATOR

SECURITY CLASSIFICATION OF THIS PAGE (When Data Entered)

REPORT DOCUMENTATION PAGE

READ INSTRUCTIONS BEFORE COMPLETING FORM

1. REPORT NUMBER: CERL-TR-M-226
2. GOVT ACCESSION NO.
3. RECIPIENT'S CATALOG NUMBER

4. TITLE (and Subtitle): LIQUID-SPRING SHOCK ISOLATOR MODELING
5. TYPE OF REPORT & PERIOD COVERED: FINAL rept. Jul 75-Aug
6. PERFORMING ORG. REPORT NUMBER
7. AUTHOR(s): P. N. Sonnenburg, B. H. Wendler, W. E. Fisher
8. CONTRACT OR GRANT NUMBER(s)
9. PERFORMING ORGANIZATION NAME AND ADDRESS: CONSTRUCTION ENGINEERING RESEARCH LABORATORY, P.O. Box 4005, Champaign, Illinois 61820
10. PROGRAM ELEMENT, PROJECT, TASK AREA & WORK UNIT NUMBERS: 4A762719AT40-A1-023
11. CONTROLLING OFFICE NAME AND ADDRESS
12. REPORT DATE: September 1977
13. NUMBER OF PAGES: 55
14. MONITORING AGENCY NAME & ADDRESS (if different from Controlling Office): 57 p.
15. SECURITY CLASS. (of this report): UNCLASSIFIED
15a. DECLASSIFICATION/DOWNGRADING SCHEDULE

16. DISTRIBUTION STATEMENT (of this Report)

Approved for public release; distribution unlimited.

17. DISTRIBUTION STATEMENT (of the abstract entered in Block 20, if different from Report)

18. SUPPLEMENTARY NOTES

Copies are obtainable from National Technical Information Service
Springfield, VA 22151

19. KEY WORDS (Continue on reverse side if necessary and identify by block number)

high-performance shock isolators
liquid spring
isolator model

20. ABSTRACT (Continue on reverse side if necessary and identify by block number)

The purpose of this pilot study was to determine whether mathematical models of high-performance shock isolators could be established from test performance data. A liquid spring was modeled using an open-parameter differential equation. A system identification technique was used to select the best algebraic form of the model and to optimize the parameters for the sample isolator. A comparison of the calculated response variables with the test data showed that the model was accurate and that isolator models could generally be established in this manner.

DD FORM 1 JAN 73 1473 EDITION OF 1 NOV 65 IS OBSOLETE

405 279

UNCLASSIFIED

SECURITY CLASSIFICATION OF THIS PAGE (When Data Entered)

Block 20 (cont'd)

The use of the isolator mathematical model and determination of optimum constant parameters for practical design purposes is discussed. However, conversion of this information to actual hardware design dimensions warrants further research and is not addressed.

FOREWORD

This investigation was conducted as part of the RDT&E Army Program 6.27[illegible], Project 4A762719AT40, "Mobility, Soils, and Weapons Effects Technology"; Task A1, "Weapons Effects and Protective Structures"; Work Unit 023, "Shock Isolation Systems for Hardened Facilities." The Technical Monitor was Mr. D. S. Reynolds, Engineering Division, Directorate of Military Construction, Office of the Chief of Engineers.

This work was carried on from July 1975 through August 1976 by the Structural Mechanics Branch (MSM), Materials and Science Division (MS), U.S. Army Construction Engineering Research Laboratory (CERL). Mr. J. Gambill set up and operated all instrumentation required for data acquisition. Mr. M. Rosenfield procured the liquid spring and monitored the design and procurement of the necessary test fixtures. Dr. W. E. Fisher is Chief of MSM, and Dr. G. R. Williamson is Chief of MS.

COL J. E. Hays is Commander and Director of CERL, and Dr. L. R. Shaffer is Technical Director.

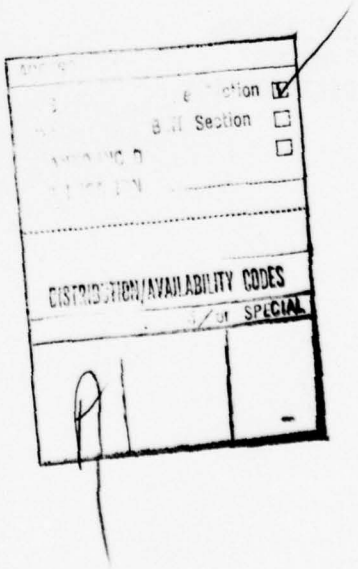

CONTENTS

FIGURES

TABLE

LIQUID-SPRING SHOCK ISOLATOR MODELING

1 INTRODUCTION

Background

Liquid-spring shock isolators are expensive, and uncertainties in judging the suitability of different isolator designs ahead of time make their procurement costly, their performance sometimes unsatisfactory, and their reliability doubtful. If mathematical models of the isolators were available from which precise design procedures could be established, however, procurement would cost less, confidence in their performance would be greater, and there would be less need to test for reliability after installation.

Four problems associated with isolation system design are the determination of (1) applied forces from expected threat conditions, (2) motion constraints imposed by equipment fragility, (3) optimum configuration of the equipment-support platform, and (4) optimum isolator performance and design. A recent report has labeled the first three problems the time optimal synthesis phase of shock-isolation system design.[1] In this synthesis, determining the force-time relationships among the isolator's elements allows one to satisfy the hardware constraints and optimize performance requirements. The lack of statistics on the loads expected and the fragility of the equipment typically make this determination difficult. This phase of design produces loading and constraint information that defines the required performance properties of the isolators.

The fourth problem has been referred to as the system-identification phase of shock isolation design.[2] In this phase, the parameters of a mathematical model of the isolator are determined so that the model's response approximates that of the isolator. If the mathematical models of isolators are in the form of differential equations containing constants, or "open" parameters, system identification methods allow one to find the optimum values of these constants. Unless such models are available, there is no way to predict performance analytically and no opportunity to control or optimize the design of isolators

---

[1] E. Sevin, et al., *Computer-Aided Design of Optimum Shock Isolation Systems*, Shock and Vibration Bulletin 39-4 (Naval Research Laboratory, 1969), pp 185-198.

[2] J. D. Collins, et al., "Methods and Applications of System Identification in Shock and Vibration," *System Identification of Vibrating Structures* (American Society of Mechanical Engineers [ASME], 1972).

through design or procurement specifications. Furthermore, knowledge of both the form of the differential equations and the optimum constant parameters is equivalent to knowledge of salient design features such as spring rate curves, damping factor curves, and isolator load capacity requirements which will provide optimum performance. Subsequently, it is necessary for the designer to convert this information into hardware design dimensions.

Because system identification methods should be useful for developing mathematical models of isolators from a limited number of simple tests, a pilot study was necessary to determine whether a model for a single isolator could be established from experimental data.

Purpose

The purpose of this report is to present the results of a pilot study to determine the feasibility of establishing mathematical models of high-performance liquid-spring shock isolators from performance test data.

Approach

Predicting isolator response under prescribed loading conditions depends on the ability to measure isolator performance mathematically. Since mathematical models are generally not available for high performance isolators, however, it was necessary to determine if limited experimental data could provide reasonably accurate models. Because it offered near-optimum response properties, a liquid-spring shock isolator with a spring rate of 400 lb/in. (70 051 N/m) and an effective linear viscous damping ratio of 0.3 was chosen. This isolator was subjected to three step pulses, from which its performance was obtained. (Such tests do not have to use realistic excitations as long as the range of motion--relative displacement, velocity, and acceleration--spans the same range as the environmental force and motion constraints.) Several nonlinear models were used to depict the spring and damping properties of the isolator.

The model's algebraic form was changed until the system-identification method, using the same forcing functions, most closely matched the model's response to the experimental data and provided optimum values for the model's coefficients. Chapter 3 gives the final form of the mathematical model, and Appendix A gives the system identification mathematics. Chapter 4 describes the comparison results, and Appendix B gives pertinent aspects of the solution method used for the model.

This report in general is directed toward finding the form of the mathematical model for a class of isolators (liquid springs) having

similar design features. The constant parameters of the model are estimated for the particular isolator used in the experiments. The spring rate and damping curves for this isolator are shown. In conventional design practice, it is highly beneficial if the mathematical model for the class of isolators is known from experiments of this type. The optimum spring and damping properties for the required platform design configuration and shock loading condition can be obtained by system-identification methods. The complete mathematical model, with optimum constants, can then be used to analytically verify performance of a design concept of the isolator and platform assembly. The final stage of converting this information into actual hardware design dimensions for the isolators is beyond the scope of this work.

Role of System Identification

System identification is a relatively new field,[3] although individual techniques associated with the field are not necessarily new. The system to be identified refers to any physical system that can be modeled mathematically. A mathematical description of the system allows analytical approximations of a system's performance.

Linear differential equations are often effective in analyzing electronic circuitry and linear mechanical vibration systems. These systems can be accurately identified using Fourier or Laplace transform techniques if the excitation and response histories are known. Linear matrix algebra, including well-known techniques such as least squares, regression analysis, Lagrange multipliers for satisfying constraints, or statistical maximum likelihood methods have been successfully used to analyze certain types of nonlinear systems, such as the problem addressed in this report. More complicated nonlinear problems may be solved using recently developed nonlinear search methods. The recognition of system identification has enabled the collection and overall review of all these techniques, however, so that the most efficient method can be developed and applied for a particular problem.

Shock isolation design provides several opportunities for applying system identification methods. Given the physical properties of the sensitive equipment and certain configuration constraints, one can design an optimum platform; given certain force and motion constraints, one can identify the optimum weighted platform design which will minimize cost. Two other possible applications of isolator design are: (1) predicting the response motions of an isolator under prescribed loading conditions, and (2) prescribing design specifications for optimum isolator performance. In the first case, a mathematical model of

[3] J. D. Collins, et al., "Methods and Applications of System Identification in Shock and Vibration," *System Identification of Vibrating Structures* (ASME, 1972).

the isolator would permit the calculation of the response from excitation information. In the second, adjusting the constants of a mathematical model allows one to obtain optimum response under given loading and motion constraints and to convert these constants to isolator design criteria. This report focuses on the first case.

Mode of Technology Transfer

The material in this report bears directly on the design and performance verification of high-performance shock isolators and shock isolation systems. The information and experience can be used in all future defense-systems development programs. The material can be used in conjunction with the following Army documentation: R. E. Crawford, J. C. Higgins, and E. H. Baltman, *A Guide for the Design of Shock Isolation Systems for Ballistic Missile Defense Facilities*, Technical Report S-23 (Construction Engineering Research Laboratory [CERL], August 1973) and incorporated into the TM 5-856 series, "Design of Structures to Resist Atomic Weapons."

2 EQUIPMENT AND TEST CONFIGURATION

Selection of the Isolator

Studies conducted for the U.S. Defense Nuclear Agency have concluded that liquid springs exhibit near-optimum response properties for high performance isolation systems.[4]

Isolator performance can be defined in terms of dissipated energy--that is, force-displacement relationships. For example, equipment fragility dictates that to insure functional survival, imposed accelerations must be limited, thus controlling the maximum force transmitted to the equipment through the isolator. Either overall or internal displacements can impair functional survival, so both types of displacement must be constrained. The dotted horizontal and vertical lines in Figure 1 indicate the performance of an ideal isolator: one that dissipates as much energy as possible.

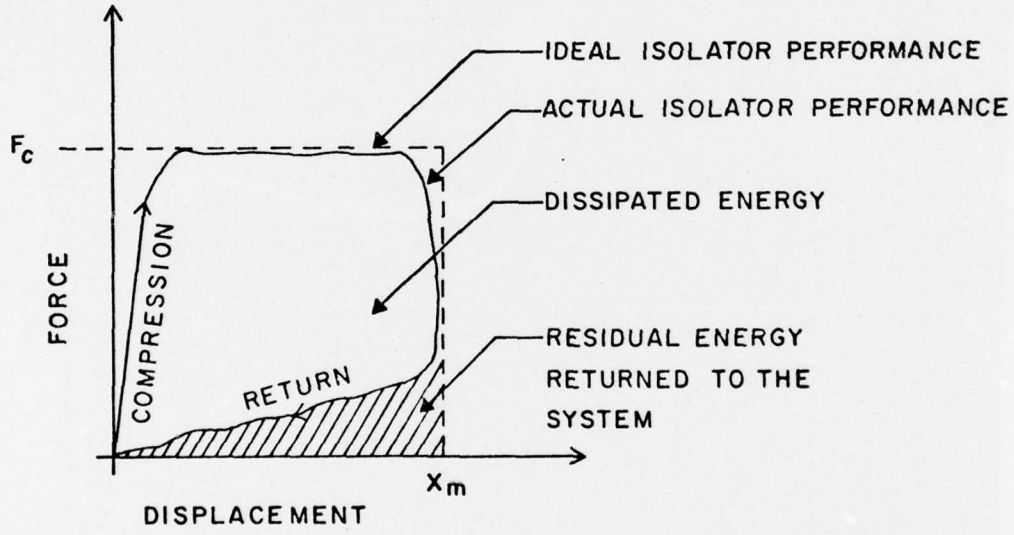

Figure 1. Force-displacement relationship for high-performance isolators.

[4] D. B. Taylor, *Application of the Hydraulic Shock Absorber to a Vehicle Crash Protection System*, Society of Automotive Engineers Paper No. 710537 (Society of Automotive Engineers [SAE], June 1971), pp 9-11.

Ideal isolators are impossible in practice because the isolator's response limits instantaneous changes in force or displacement states. The solid line in Figure 1 illustrates the force-displacement properties of a high-performance liquid-spring shock isolator. Figure 2 illustrates the force-displacement properties for the device tested in this project.[5]

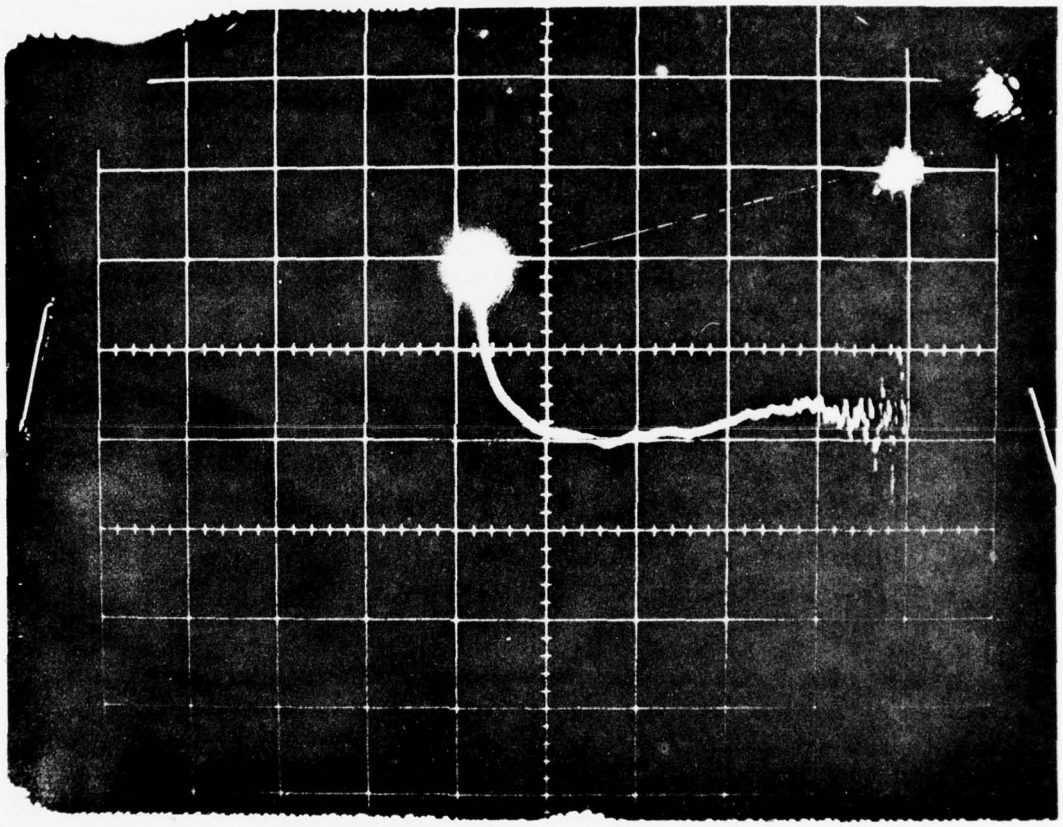

Figure 2. Force-displacement relationship for the tested liquid-spring shock isolator.

[5] *Investigation of Optimum Passive Shock Isolation Systems*, Technical Report No. AFWL-TR-72-148 (Air Force Weapons Laboratory, 1973), p 154.

The fluid compressibility, viscosity, and mechanical and fluid friction determine the response of liquid spring isolators. Compression of the silicone fluid with a variable diameter piston rod provides the spring effect (Figure 3a); fluid flow around the piston provides the major source of damping (Figure 3b).

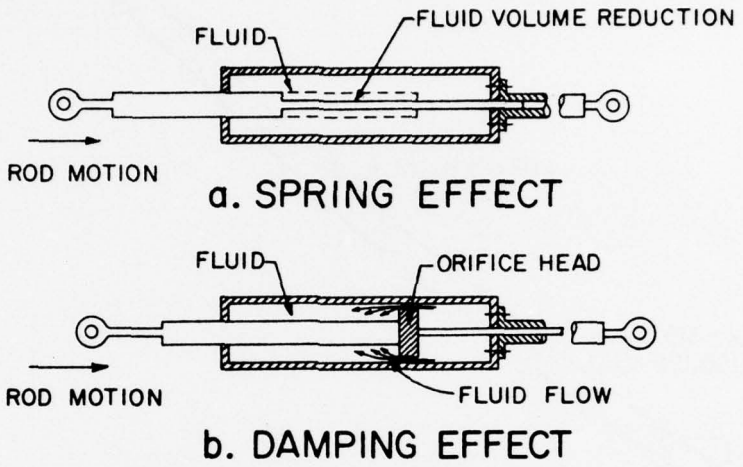

Figure 3. Characteristics of a liquid-spring shock isolator.

A liquid-spring shock isolator was used in a simple test to provide data for optimizing the coefficients of the mathematical model. The isolator met performance specifications requiring a spring rate of 400 lbs/in. (70 051 N/m), an effective linear viscous damping ratio of 0.3, and a 12-in. (0.305-m) stroke. Static tests by the manufacturer indicated a spring rate of 315 lbs/in. (55 165 N/m) for small displacements and 546 lbs/in. (95 619 N/m) at full stroke (Figure 4). Chapter 3 further discusses the hardening exhibited by this static spring.

The manufacturer's tests indicated an equivalent viscous damping coefficient of 0.28 to 0.43, varying with velocity. Thus damping was nonlinear, as expected.

The manufacturer suggested that the dynamic spring rate and damping coefficient would exhibit *softening* (see Chapter 3), even though static tests showed *hardening*. This statement simply implies, however, that the dynamic properties were generally different from those the manufacturer had equipment to measure.

Because it can perform in both directions, the liquid spring isolator is a complex mechanism, as shown in Figure 5.

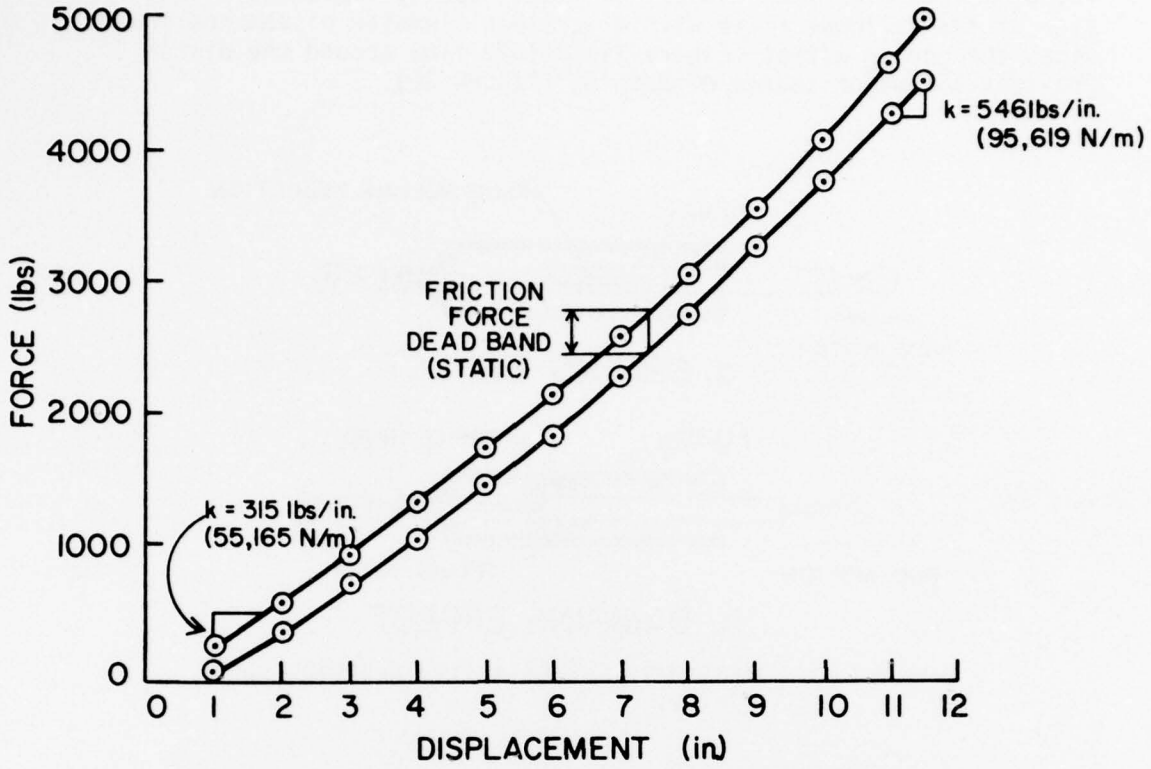

Figure 4. Static spring-rate curve for the test isolator.

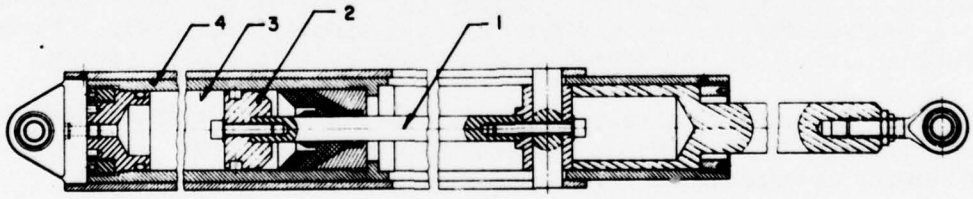

1. Piston rod
2. Double-walled sealed container
3. Piston
4. Silicone fluid

Figure 5. Sectional view of test isolator.

Test Configuration

The least-squares system-identification technique requires measured input motion (base displacement), measured output response (mass displacement), and an open-parameter differential equation as a trial mathematical model of the isolator. This method is most accurate when the isolator is tested through its entire displacement range (12 in. [0.305 m]), with relative velocities in excess of 100 in./sec (2.54 m/s).

The test configuration, shown in Figure 6, provides the maximum relative displacement and velocity using available test fixtures. One end of the liquid spring was attached to a rigid base mounted on the CERL Biaxial Shock Test Machine (BSTM) test platform and the other end was attached to a 6000-lb (2722-kg) mass. Rollers supported the mass and allowed it to move in only the horizontal plane. Rolling friction was not significant. Base displacement was applied to the isolator through the rigid base mounted on the test platform.

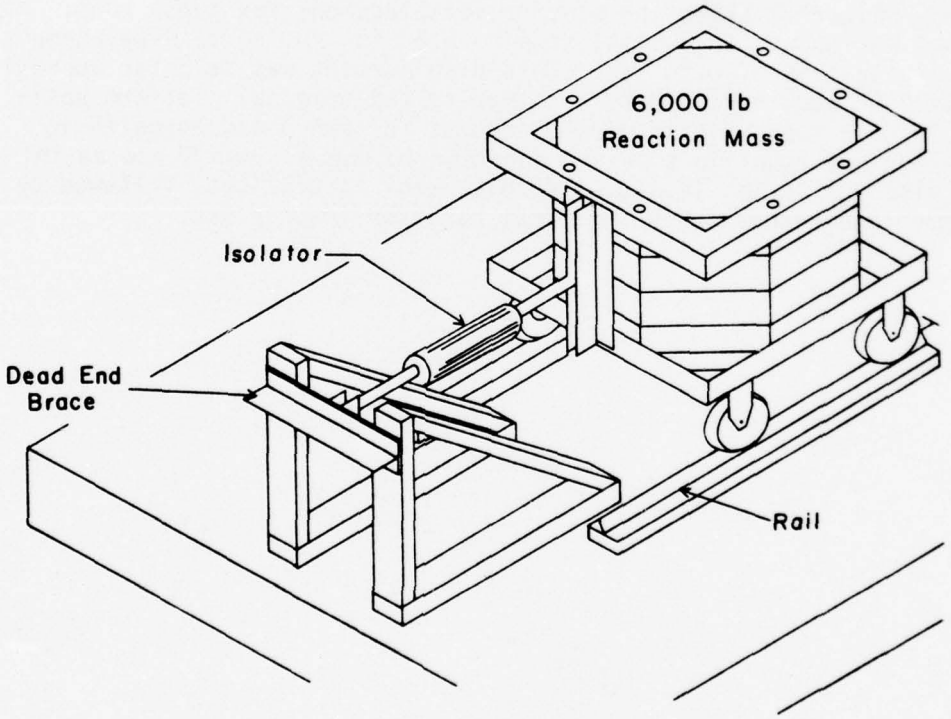

Figure 6. Test carriage on liquid-spring mounting frame.

Six uniaxial electrohydraulic actuators, with a total capacity of 450,000 lbs (2 001 700 N) provided the horizontal motion. The actuators drive the 12-ft square (3.658-m square) all-welded aluminum test platform. A pressurized hydraulic fluid provided the excitation energy, and a 330-gpm (0.0208 m^3/s) servovalve on each actuator controlled it. Figure 7 shows a functional diagram of the control system.

Optical-electronic equipment provided the excitation and mass response displacement data. Differentiating the displacement data yielded the velocity and acceleration. All data were recorded on analog tape, then digitized and filtered for reduction.

Base Excitation Motions

A series of preliminary sinusoidal tests to determine adequate mass response showed a gradual increase in relative response amplitude, caused by a rapid rise in isolator fluid temperature and a decrease in fluid viscosity. These results caused the steady-state testing to be abandoned.

Three transient tests, labeled runs A, B, and C, were then performed. Figure 8 shows the platform displacement for these runs. Run A input motion was an initial step to 5.50 in. (0.140 m) displacement with a rise time of 0.20 sec. This displacement was held for approximately 2.00 sec, followed by a return to the original platform position in 0.12 sec. Platform displacement for run B was opposite in direction but equal in size and duration to run A. Run C had an initial rise to 5.5 in. (0.140 m) displacement in 0.12 sec, followed by an immediate return to the original position in 0.12 sec.

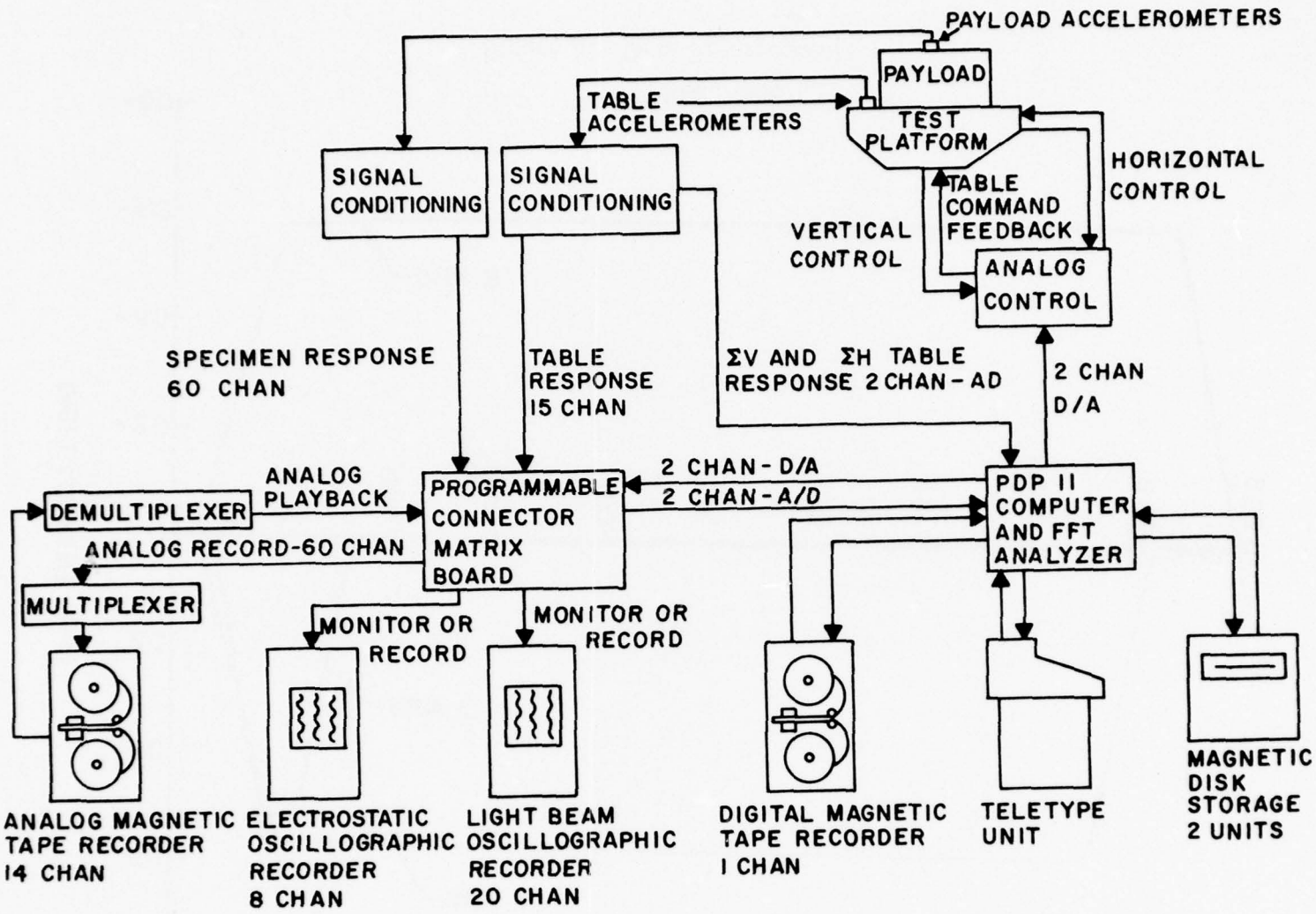

Figure 7. Flow chart of control and payload instrumentation systems.

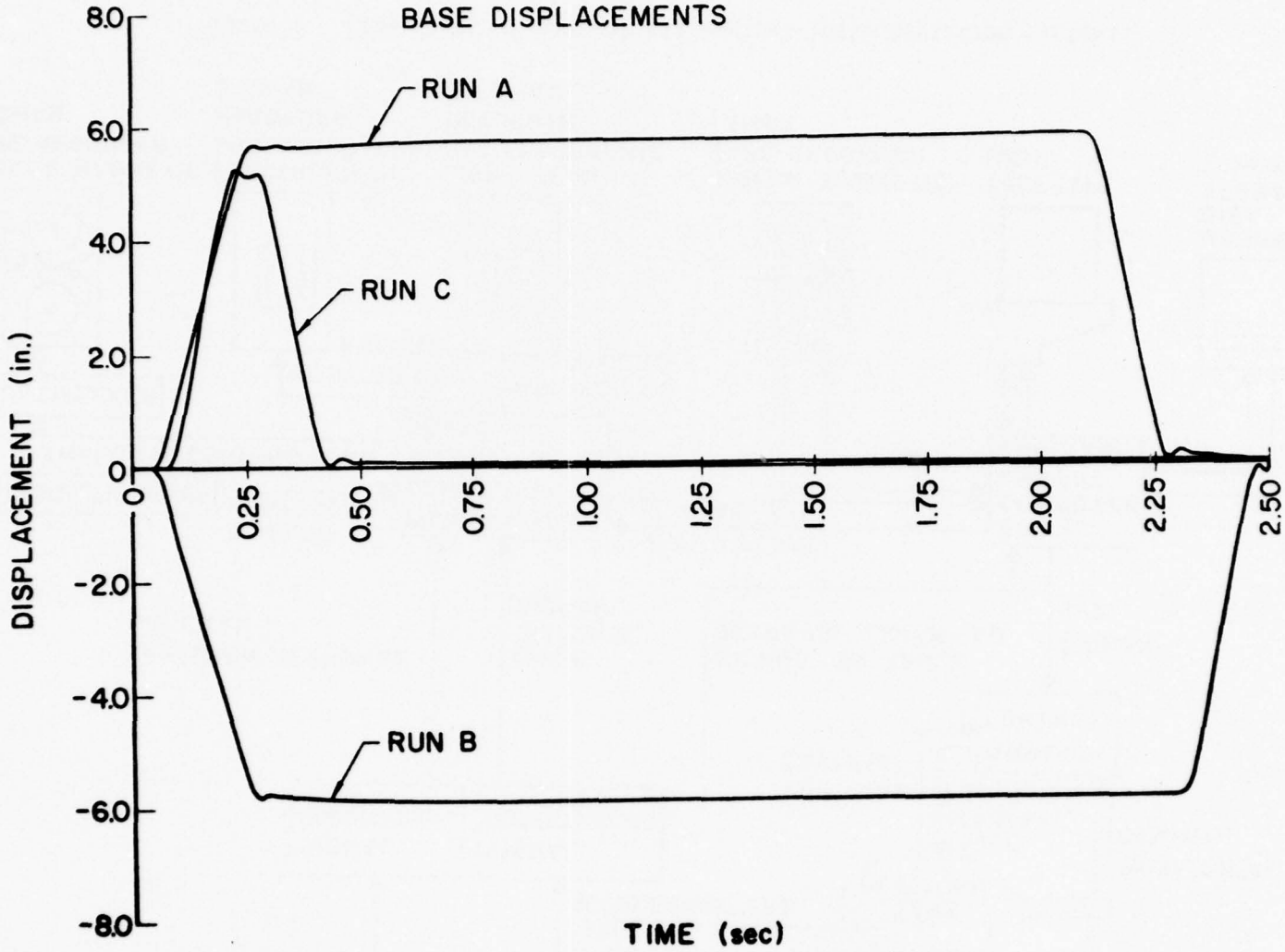

Figure 8. Base displacements.

3 FORMULATION OF THE MATHEMATICAL MODEL

Physical and Mathematical Properties

Liquid springs behave like automotive shock absorbers. Figure 9a shows a simplified, single-acting liquid spring. Motion of the rod to the right will cause a spring effect by fluid compression, and a damping effect by flow of fluid through or around the orifice head. This isolator can (1) dissipate energy efficiently by fluid damping, and (2) return to original length after distortion. The latter property causes some loss of efficiency from energy dissipation, but it is a practical necessity.

Figure 9b shows a free-body model of the isolator. F(t) represents the action and reaction forces applied externally to the isolator. The internal force causing the compressed isolator to return to its original position is shown as a spring, and is depicted mathematically as $f_1(z)$. This spring is a potential energy force, and is a function of piston position. The internal force causing damping is shown as a dashpot, and is depicted mathematically as $f_2(\dot{z})$. This dashpot is a nonconservative force, for it removes energy from the mechanical system (the isolator) by converting it into heat, which is dissipated to the surrounding air. The mathematical model for the isolator is:

$$F(t) + f_1(z) + f_2(\dot{z}) = 0. \qquad \text{[Eq 1]}$$

Either the spring or the fluid damping can exhibit hardening or softening properties, as illustrated in Figure 10.[6,7] Hardening occurs when the internal force increases more rapidly than the displacement or velocity. Softening occurs when the internal force increases less rapidly than the displacement or velocity. By requiring both $f_1(z)$ and $f_2(\dot{z})$ to soften as in Figure 1, one can cause the most energy to be dissipated most quickly. Optimizing the precise shape of the softening curves for each of these functions and for each isolation system allows one to maximize the energy dissipation efficiency.

Several practical design features such as displacement dead space, fluid preloading, and static friction, can influence the shape of the

---

[6] W. J. Cunningham, *Introduction to Nonlinear Analysis* (McGraw-Hill, 1958), p 76.

[7] S. Timoshenko, D. H. Young, and W. Weaver, *Vibration Problems in Engineering* (John Wiley and Sons, 1974), p 163.

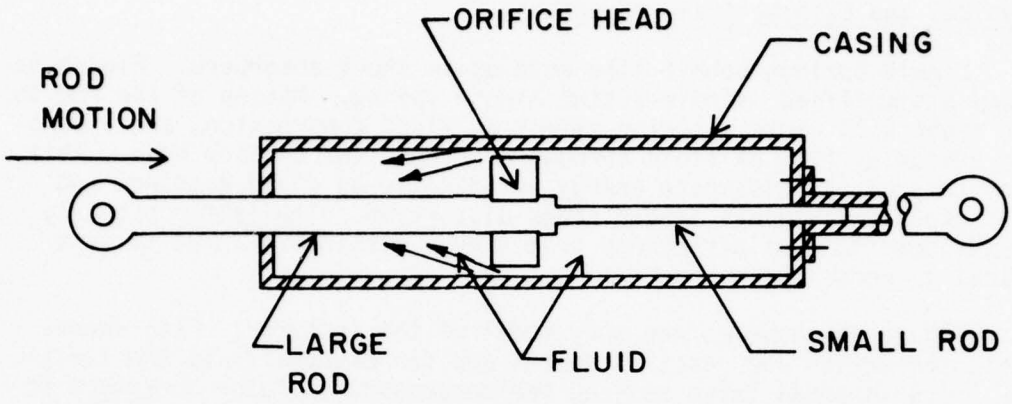

A. DIAGRAM OF A SINGLE ACTING LIQUID SPRING SHOCK ISOLATOR

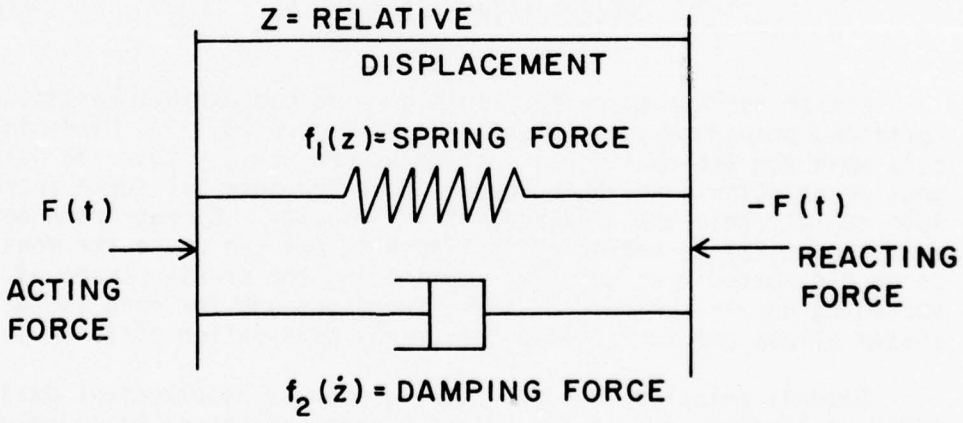

B. FREE BODY DIAGRAM OF ISOLATOR

Figure 9. Simplified diagrams of liquid-spring shock isolator.

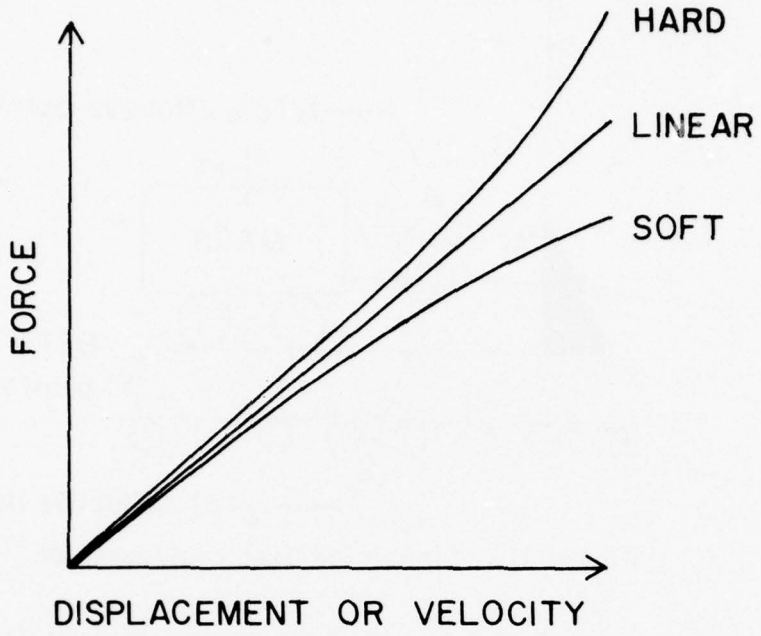

Figure 10. Hardening and softening properties.

curves for $f_1(z)$ and $f_2(\dot{z})$. Displacement dead space results from little or no resistance to motion in the vicinity of $z = 0$, and is not directly associated with the frictional dead space shown in Figure 4. Under dynamic operating conditions, frictional dead space will appear as a constant friction damping term in $f_2(\dot{z})$. An air bubble or void in the fluid chamber can cause a dead space in displacement. Preloading a liquid spring can slightly modify the shapes of $f_1(z)$ and $f_2(\dot{z})$ in addition to modifying the spring's response at small displacement velocities. However, preloading is impossible if there is a void in the fluid chamber, for static friction will create a minimum applied force before the relative motion of the isolator starts. The section on Nonlinear Spring and Damping Effects discusses the mathematical aspects of these features.

General Formulation of the Model

Figure 11 shows a simplified model of the test configuration. The coordinate, x, is the absolute displacement of the mass, m; absolute table displacement, u, causes the forces applied to the mass. The relative displacement between the mass and the table is $z = x - u$. Likewise, the relative velocity is $\dot{z} = \dot{x} - \dot{u}$, where the superimposed dot means differentiation with respect to time.

The spring and damper effects represent the isolator's behavior. Spring forces that restore the mass to equilibrium are represented by

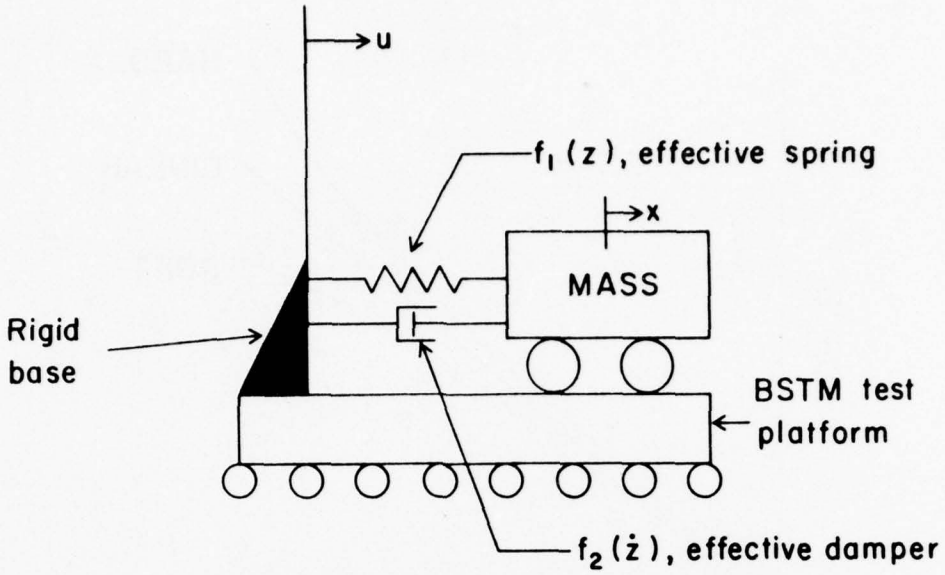

Figure 11. Simplified test configuration.

$f_1(z)$, which is a nonlinear function of z. Forces that dissipate energy are represented by $f_2(\dot{z})$, which is a nonlinear function of $\dot{z}$. The forces applied to the isolator, which constitute the F(t) term in Eq 1, are caused by the table motion and the inertia of the mass.

Identification of Applied Forces

For an isolator with linear elasticity and damping, the mathematical model is:[8]

$$m\ddot{z} + kz + c\dot{z} = m\ddot{u} \qquad \text{[Eq 2]}$$

where k and c are constants, i.e., $f_1(z) = kz$ and $f_2(\dot{z}) = c\dot{z}$. Thus, $-m\ddot{u}$ appears on the right side as a forcing function. The same form of the differential equation is approximate when $f_1(z)$ and $f_2(\dot{z})$ are nonlinear, whereby:

$$m\ddot{z} + f_1(z) + f_2(\dot{z}) = -m\ddot{u}. \qquad \text{[Eq 3]}$$

Substituting $\ddot{x} = \ddot{y} + \ddot{u}$ yields

$$m\ddot{x} = f_1(z) + f_2(\dot{z}) = 0. \qquad \text{[Eq 4]}$$

[8] S. H. Crandall and W. D. Mark, *Random Vibration in Mechanical Systems* (Academic Press, 1963), p 62.

Equations 1 and 4 are the same, for $F(t) = m\ddot{x}$.

Nonlinear Spring and Damping Effects

The nonlinear terms $f_1(z)$ and $f_2(\dot{z})$ can be expressed to any desired degree of accuracy by expanding orthogonal functions. For example, for a sufficiently large number of terms, N, the following expansion can represent either a hardening or softening spring:

$$f_1(z) = \sum_{n=1}^{N} k_n z^n \qquad \text{[Eq 5]}$$

where n is an integer, and k_n is a constant. Accumulating more than a few terms for either $f_1(z)$ or $f_2(\dot{z})$, however, would result in awkward and time-consuming calculations. Although in theory, short power-series expansions can model either softening or hardening, in practice, unstable solutions result when large motions are modeled.

The use of powers less than unity is a possible way to depict softening:

$$f_1(z) = k_1 z + k_2 z^a \qquad \text{[Eq 6]}$$

where $0 \leq a < 1$. The slope in Eq 6 is:

$$\frac{df}{dz} = k_1 + k_2 a z^{a-1} \qquad \text{[Eq 7]}$$

which becomes infinite for $z = 0$. An infinite slope at $z = 0$ is the same condition as a preloading effect, discussed below. To obtain damping properties, one can model an infinite slope at $z = 0$ using a coulomb friction effect, also discussed below. This type of expansion was tried for both $f_1(z)$ and $f_2(\dot{z})$ with generally poor results because the two effects were not sufficiently independent of other effects being modeled. Note that Eq 6 does not generally represent an orthogonal expansion.

The hyperbolic tangent provides an appropriate representation for softening:[9]

$$f_1(z) = k_1 z + k_2 \tanh(\alpha z). \qquad \text{[Eq 8]}$$

[9] S. Timoshenko, D. H. Young, and W. Weaver, *Vibration Problems in Engineering* (John Wiley and Sons, 1974), p 167.

A similar expression can represent damping, except that the equation includes a term for coulomb friction:

$$f_1(\dot{z}) = c_1\dot{z} + c_2 \tanh(\beta\dot{z}) + c_3 \operatorname{sgn}(\dot{z}). \qquad \text{[Eq 9]}$$

In Equations 8 and 9, α and β are constants, while $\operatorname{sgn}(\dot{z}) = \pm 1$, according to the algebraic sign of $\dot{z}$.

Discussions with the manufacturer indicated that response results might reflect the effects of displacement, dead space, and preloading. All these conditions affect the form of either $f_1(z)$ or $f_2(\dot{z})$ in the neighborhood of $z = 0$. Figure 12a shows the effect of dead space--no resistive force--for $z = \pm\delta$. Figure 12b shows the effect of preloading--an instantaneous positive or negative force--for $f_1(z) = \pm\gamma$ at $z = 0$. Actually, the combination of these effects was evident, as shown in Figure 12c, even when γ was negligible (see Chapter 4). The isolator used in these experiments contained a narrow-band amplifier type of orifice head,[10] so the computer model was adjusted to account for this effect.

Finally, the effect of static friction was included in the model. Trials with the coulomb friction term (in which a constant friction force occurs at all velocities) in Equation 9 poorly duplicated this behavior. Hence equivalent static friction was included, and was automatically actuated within the maximum observed band of residual displacement whenever $|\dot{z}| \leq \varepsilon$, where ε is a small constant.

Final Model and Supporting Rationale

All the mathematical forms mentioned in the previous subsection were tried. The least-squares method of system identification was used to find optimum values of k_1, k_2, c_1, c_2 and c_3. These constants, which constitute the unknowns in a set of simultaneous linear algebraic equations, are optimized using the techniques described in Appendix A. The constants α, β, γ, δ, and ε, which appear within the nonlinear expressions of z and $\dot{z}$, were independent values obtained from the experimental data, and were thus optimized by trial and error. Because the least-squares method yields an overall variance and a covariance matrix (see Appendix A), the Greek constants could be optimized quickly in several iterations by selecting values which would minimize the variance while permitting good conditioning of the covariance matrix. Good conditioning of the covariance matrix, in turn,

[10] D. B. Taylor, *Applications of the Hydraulic Shock Absorber to a Vehicle Crash Protection System*, Society of Automotive Engineers Paper No. 710537 (SAE, June 1971), pp 6,7.

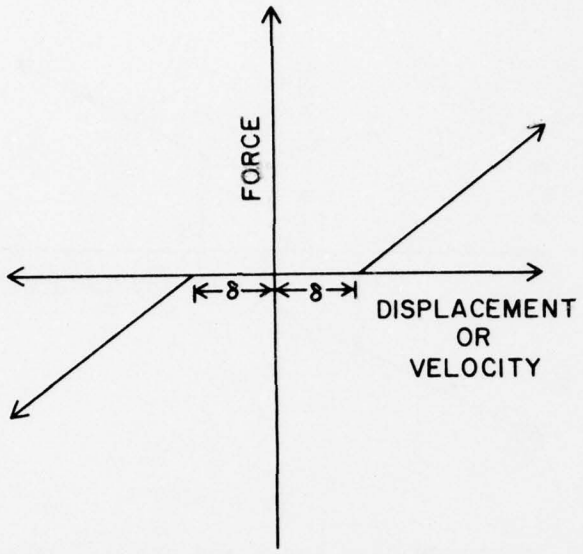

a. Dead space effect.

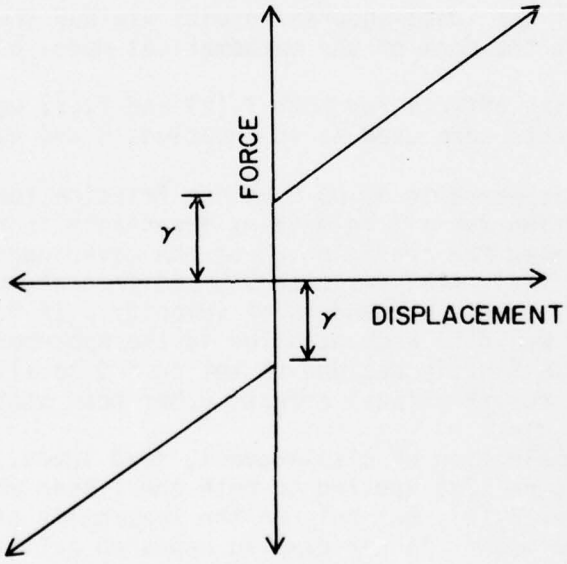

b. Preload effect

Figure 12. Dead space and preload effects on spring rate.

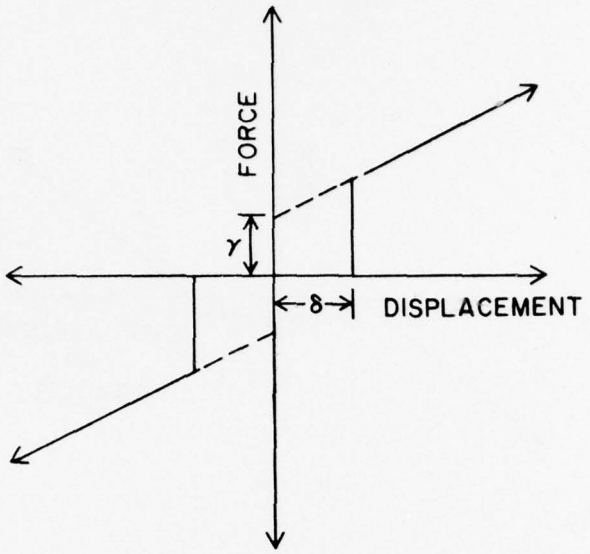

c. Combined dead space and preload effects

Figure 12. (Cont'd)

implies that the form of the mathematical model was appropriate, since the nonlinear terms would be relatively independent of each other.

Analysis of the least-squares results yielded the following observations about the form of the mathematical model of the isolator:

1. Softening effects for both $f_1(z)$ and $f_2(\dot{z})$ were clear, so hyperbolic tangents were used as in Equations 8 and 9.

2. There appeared to be no constant friction force. Inclusion of coulomb friction for all velocities invariably increased the variance and decreased the conditioning of the covariance matrix. This result does not imply that friction was not present, but rather that it was most likely not independent of velocity. If friction depended on velocity, it would be accounted for in the hyperbolic tangent term of $f_2(\dot{z})$. It was finally decided to set $c_3 = 0$ to allow the $\tanh(\beta\dot{z})$ term to account for frictional effects other than static friction.

3. The combination of displacement, dead space, and preloading (as shown in Figure 12c) applied to both the linear and the hyperbolic tangent terms for $f_1(z)$, but only to the hyperbolic tangent term for $f_2(\dot{z})$. In other words, linear damping appeared active in the dead space, while the remaining terms provided no resistance to motion. Furthermore, the value of γ associated with preloading was found to be

negligible--a result verified as likely by the manufacturer[11]--for two reasons. First, the initial preloading fluid pressure provided by the manufacturer was relatively low. Second, because the isolator had been operating for extended periods at high fluid temperatures, it had leaked some fluid. In either case, a void in the fluid chamber could be expected.

The observations led to a definition of the best mathematical model for the isolator in the form of Equation 1 as

$$F(t) + k_1 z + k_2 \tanh(\alpha z) + c_1 \dot{z} + c_2 \tanh(\beta \dot{z}) = 0. \quad \text{[Eq 10]}$$

Equation 10 shows that

$$f_1(z) = k_1 z + k_2 \tanh(\alpha z) \quad \text{[Eq 11]}$$

$$f_2(\dot{z}) = c_1 \dot{z} + c_2 \tanh(\beta \dot{z}). \quad \text{[Eq 12]}$$

The results of applying Equation 10 to the physical model for the test configuration (replacing $F(t)$ with $m\ddot{x}$) are presented in the following section. The actual table displacement was used as the base motion excitation for both models. Appendices A and B discuss techniques for treating the special effects of dead space and static friction.

[11] CERL Telephone Memorandum from B. Wendler to Taylor Devices, Inc., dated 25 August 1976.

4 RESULTS

Average Parameter Values

The coefficient parameters k_1, k_2, c_1, and c_2 with $c_3 = 0$) in Equation 10 were calculated and optimized by the least-squares method. Nonlinear parameters (those denoted by lower-case Greek letters) could not be optimized in this manner. Although it would have been desirable to optimize the nonlinear parameters automatically, more programming time would have been needed, so these parameters were adjusted by trial and error, using the overall variance and the covariance matrix conditioning as indicators of improvement (see Appendix A). Solutions were always highly stable[12] in that small changes in constant parameters yielded small changes in response.

Table 1 gives the optimized constants for all three tests; averages are in the far right column of the table. The constants for tests A and B appear to agree fairly closely, although k_2 and c_2 for run C are somewhat high. Table 1 allows comparison of the experimental response variables of relative displacement and velocity and absolute mass acceleration, with the corresponding theoretical values of the same variables calculated using the average constants. Such a comparison should demonstrate the stability of the theoretical solution of the mathematical model.

The graphs in Chapter 2 show the table motions, u(t), for the three tests selected for analysis. Changes in the viscous properties for run C are explainable, given the sensitivity of liquid springs to changes in fluid temperature.[13] Test C was run after about ten previous tests in close succession, which raised the temperature of the fluid enough to render the isolator casing warm to the touch.

Comparison of Model Solutions With Experimental Data

A comparison of some preliminary model predictions with experimental data demonstrates that the least-squares technique can generate optimum constants for the mathematical model. Figures 13a, b, and c show the comparison of the variables (relative displacement and

---

[12] R. Courant and D. Hilbert, "Methods of Mathematical Physics," Vol II, *Partial Differential Equations* (John Wiley and Sons, 1962), p 227.

[13] R. E. Crawford, C. J. Higgins, and E. H. Baltman, *A Guide for the Design of Shock Isolation Systems for Ballistic Missile Defense Facilities*, Technical Report S-23 (Construction Engineering Research Laboratory, 1973), p 247.

Table 1

Optimized Constants

Constant	Run A	Run B	Run C	Average
k_1 lb/in.	439	388	389	405
k_2 lb	122	154	366	214
c_1 lb/in./sec	36.8	43.5	22.9	34.4
c_2 lb	359	293	910	520
c_3 lb	0	0	0	0
α	2	2	2	2
β	2	2	2	2
γ lb	0	0	0	0
δ in.	0.77	0.77	0.77	0.77
ε in./sec	0.60	0.60	0.60	0.60

velocity and absolute mass acceleration) for test A, using the optimum constants generated for test A.

Agreement is sufficiently accurate in Figures 13a, b, and c to conclude that the mathematical model depicts the behavior of the isolator for test A. The large oscillations in the acceleration trace of the real data in Figure 13c are attributable to experimental noise, since the measured displacement trace is differentiated twice to obtain acceleration. The pulse at point A in Figure 13c is the sudden actuation of the $\tanh(\beta\dot{z})$ term (nonlinear damping) in Equation 10 when motion is somewhat mild and the relative displacement has exceeded the dead band. Only linear viscous forces have been observed to be active in the dead band, where $|z| \leq \delta$. The model would be even more accurate if this pulse (point A) had occurred slightly earlier, to match the real data at about point B in the figure. Although no time was spent matching the slow motion of the isolator near the dead band with any greater accuracy, it should not be difficult to adjust the model for better agreement. For high-performance shock isolation, accurate prediction of terminal motion around the dead band is unnecessary.

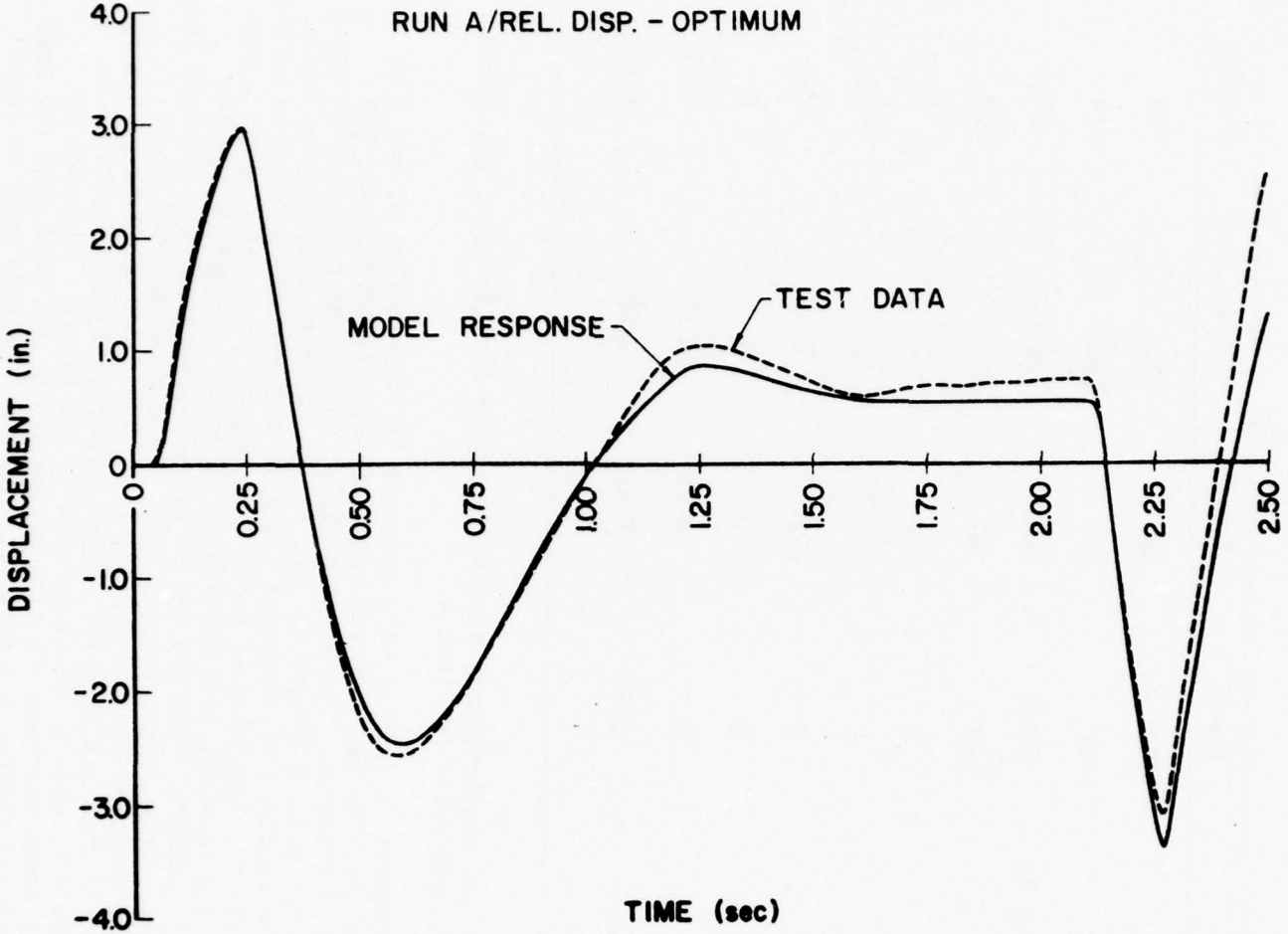

a. Relative Displacement.

Figure 13. Run A--optimum constants.

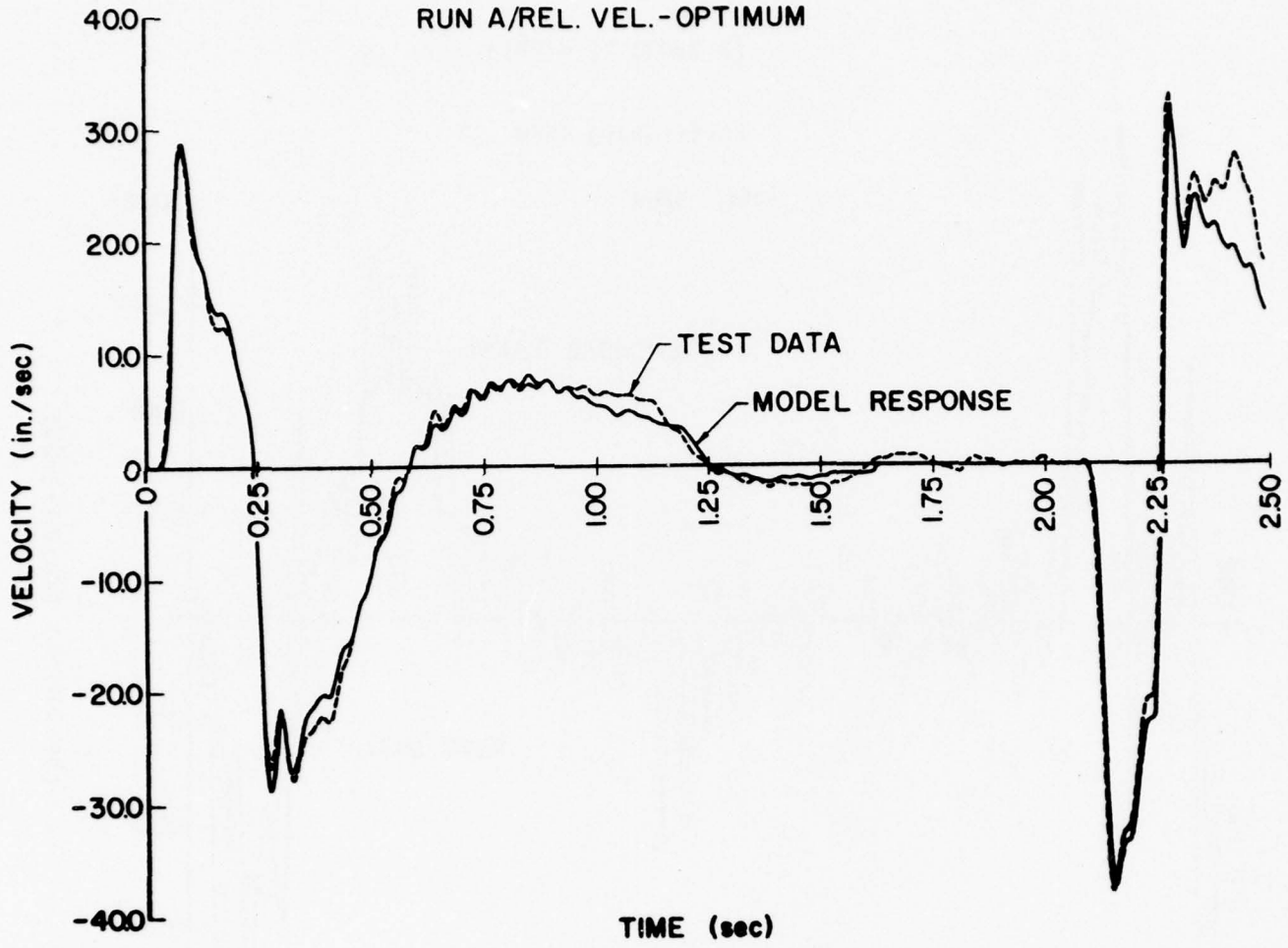

b. Relative Velocity.

Figure 13 (cont'd)

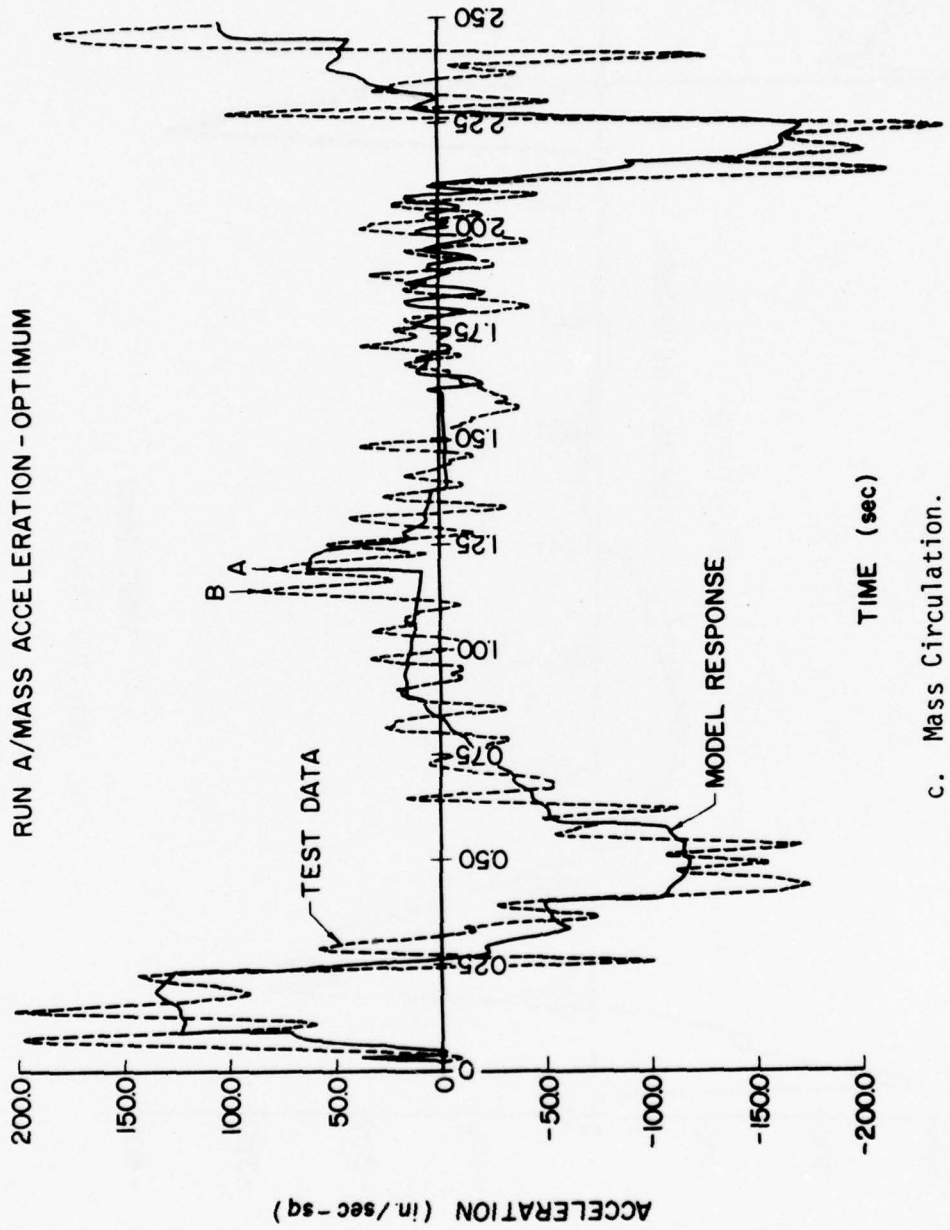

c. Mass Circulation.

Figure 13 (cont'd)

In Table 1, the average values of the constants (the far right column of values) are somewhat different than the optimum values found for test A. In particular, k_2 is 75 percent higher, and c_2 is 45 percent higher. As previously discussed, the rather large changes in these constants are attributable to the weighting effect of those values optimal for test C. Figures 14a, b, and c show the effect of using the average constants, using test A again for the comparison. The effect is slightly less agreement than in the optimal plots for test A (Figures 13a, b, and c). Thus the theoretical solutions are stable.

The significant conlusion of this research is that the constant parameters do not have to be specified precisely in order to obtain reasonably accurate predictions of response properties. This is a highly desirable result, since minor design-tolerance differences between nominally identical isolators in practical applications will cause the constants for optimal models to be slightly different. Therefore, average values for these constants should predict response properties that reasonably approximate actual response properties.

Figures 15a, b, and c compare the response variables for test B, using the average constants from Table 1. Figures 16a, b, and c show the same type of results for test C, again using the average constants instead of the optimal constants for that test.

Finally, Figures 17 and 18 show the nonlinear spring and damping curves calculated from Equations 11 and 12 for $f_1(z)$ and $f_2(\dot{z})$, using the averaged constants from Table 1.

The results discussed above were obtained from only three tests, one of which was held with elevated fluid temperature. Averaging more tests and more closely controlling test conditions should yield even better results.

For the purposes of this work, establishing mathematical models for high-performance isolators from experimental data is feasible.

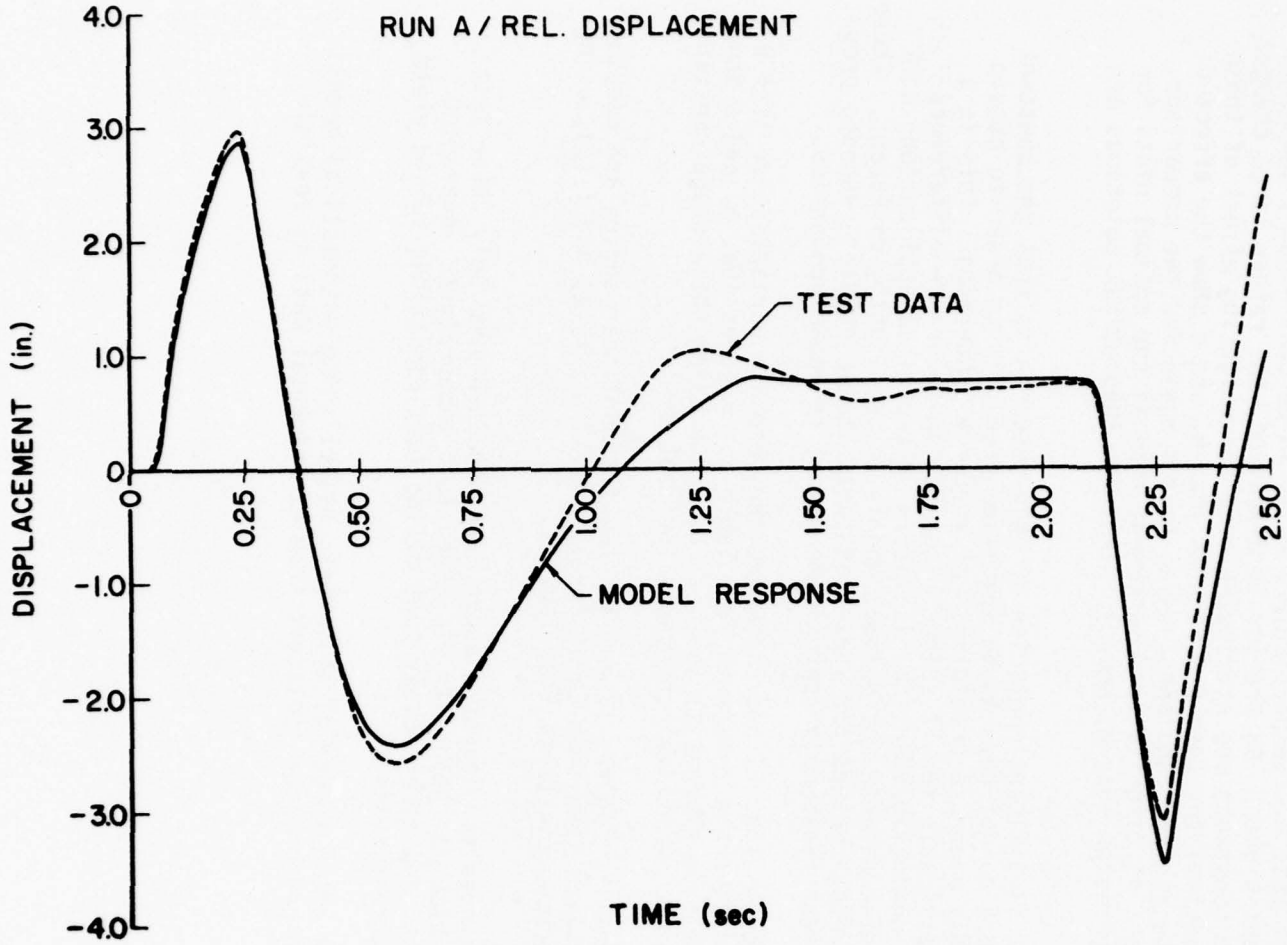

a. Relative Displacement.

Figure 14. Run A--averaged constants.

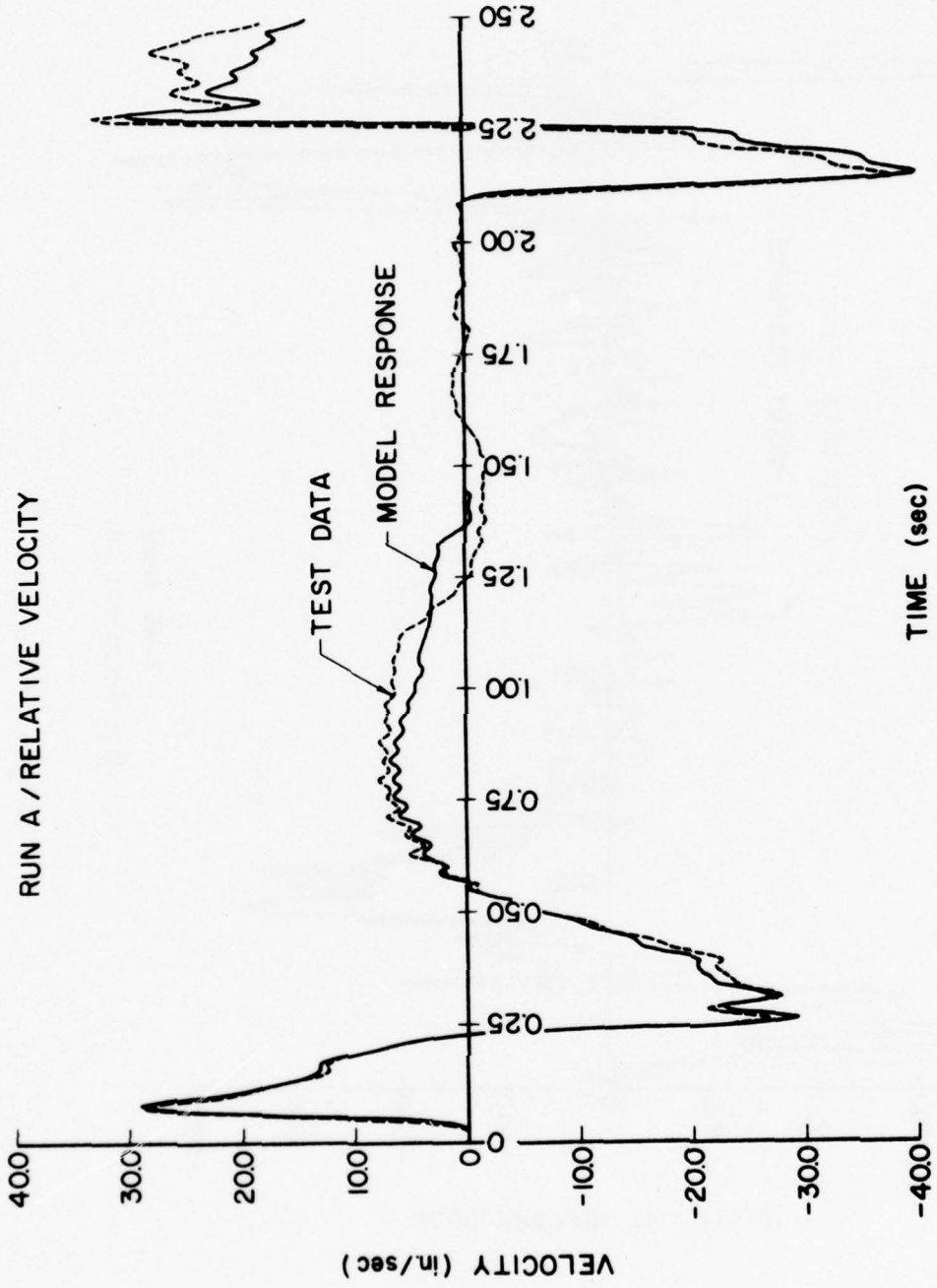

b. Relative Velocity.

Figure 14 (cont'd)

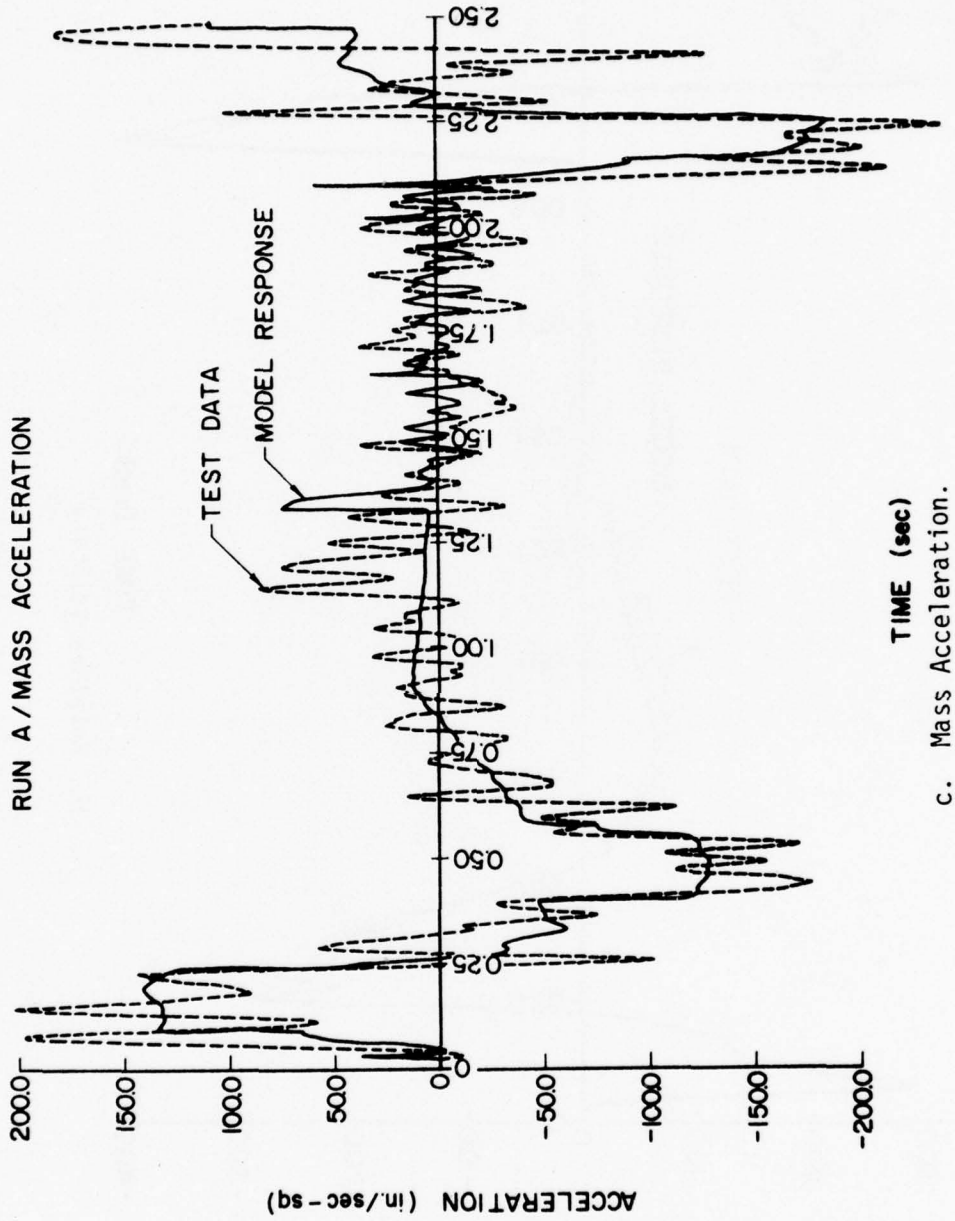

c. Mass Acceleration.

Figure 14 (cont'd)

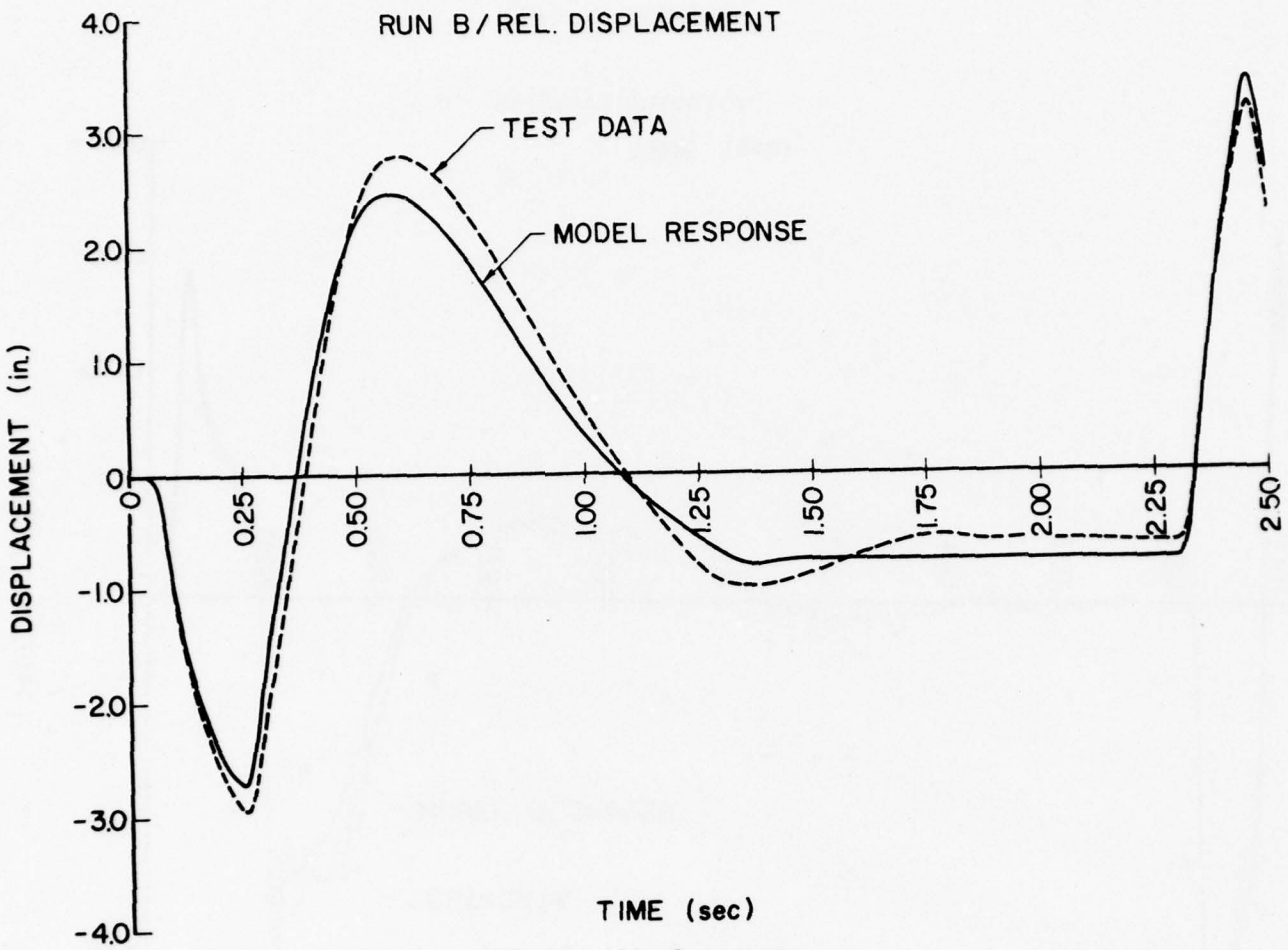

a. *Relative Displacement.*

Figure 15. Run B--averaged constants.

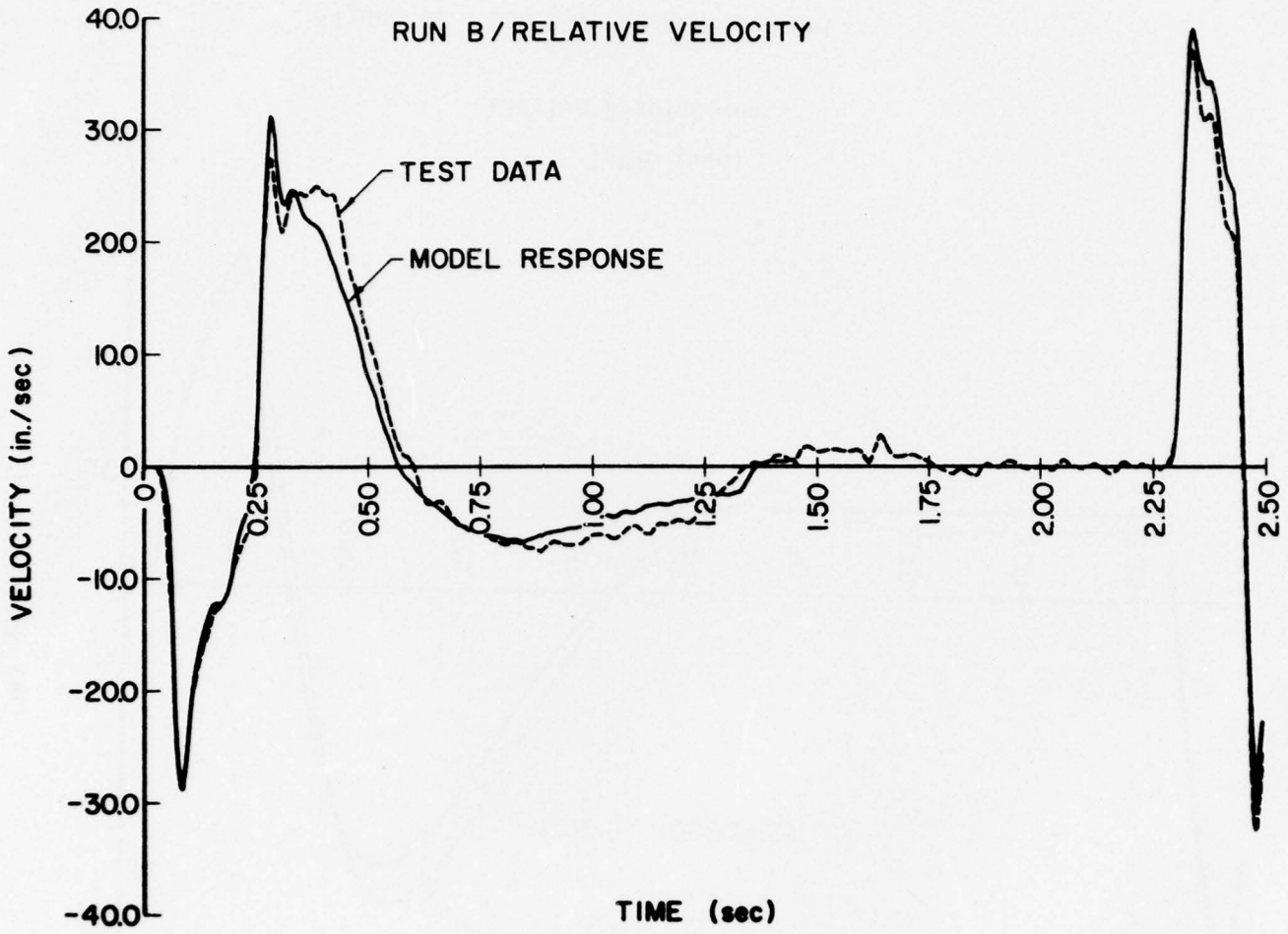

b. Relative Velocity.

Figure 15 (cont'd)

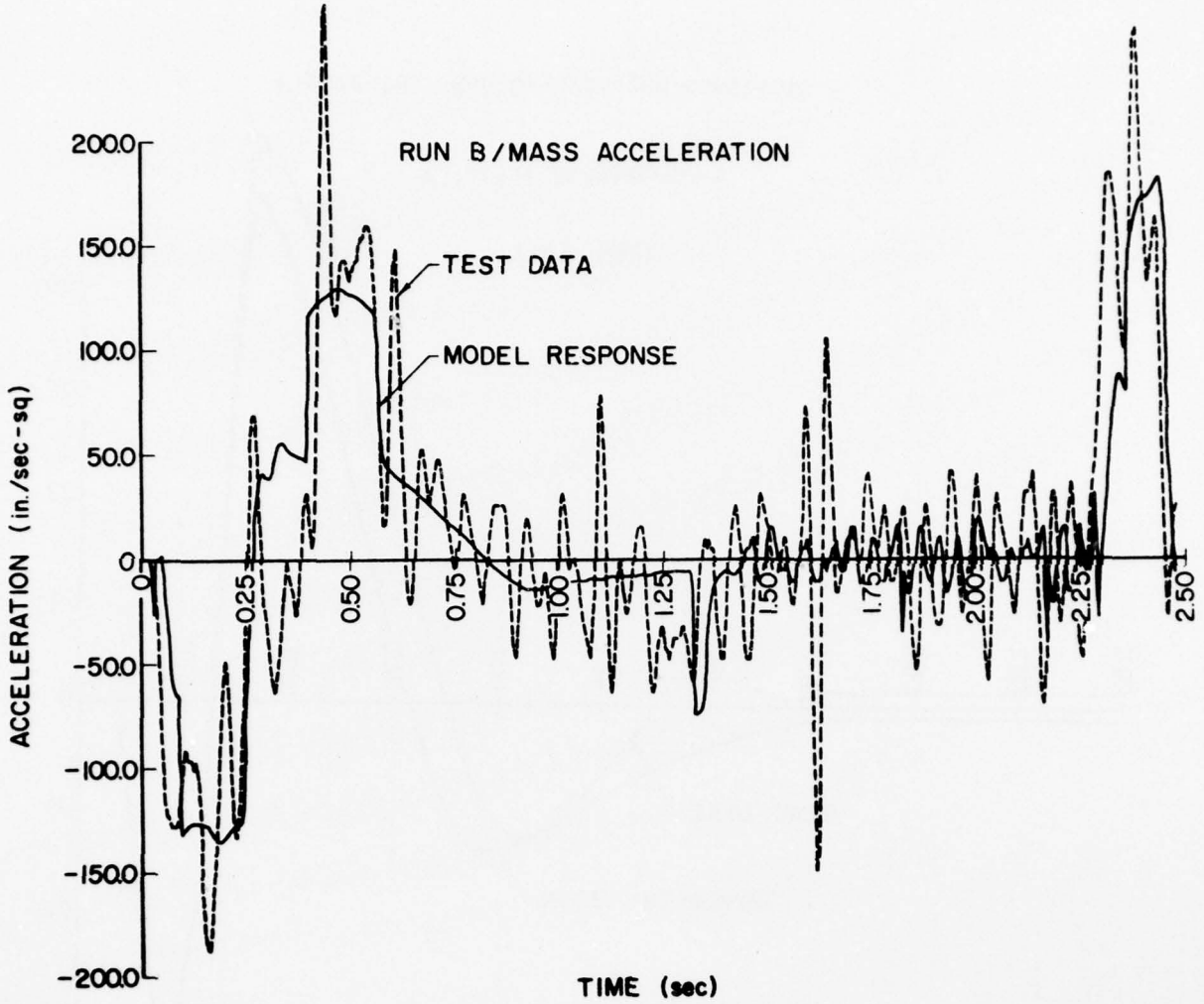

c. Mass Acceleration.

Figure 15 (cont'd)

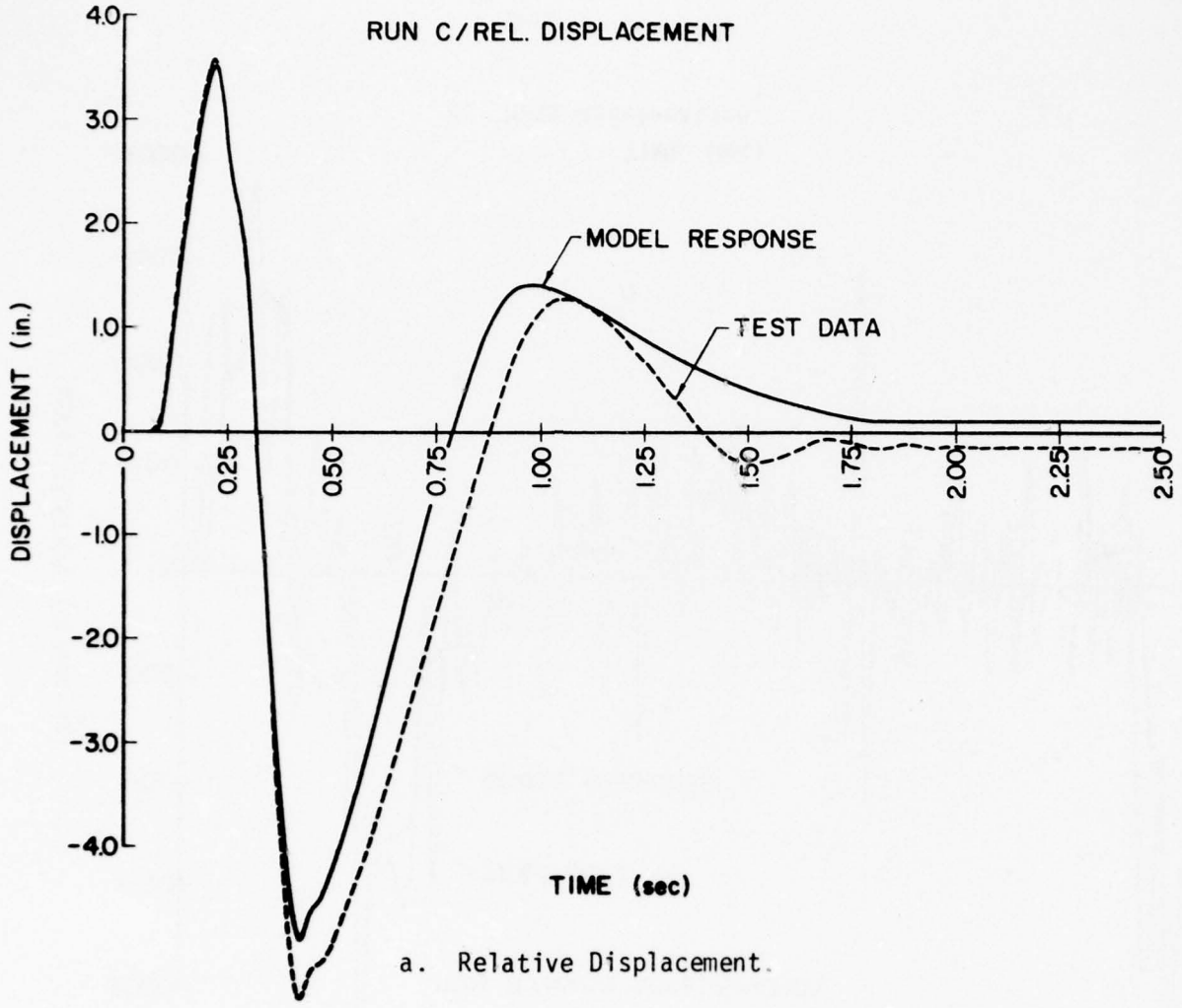

a. Relative Displacement.

Figure 16. Run C--averaged constants.

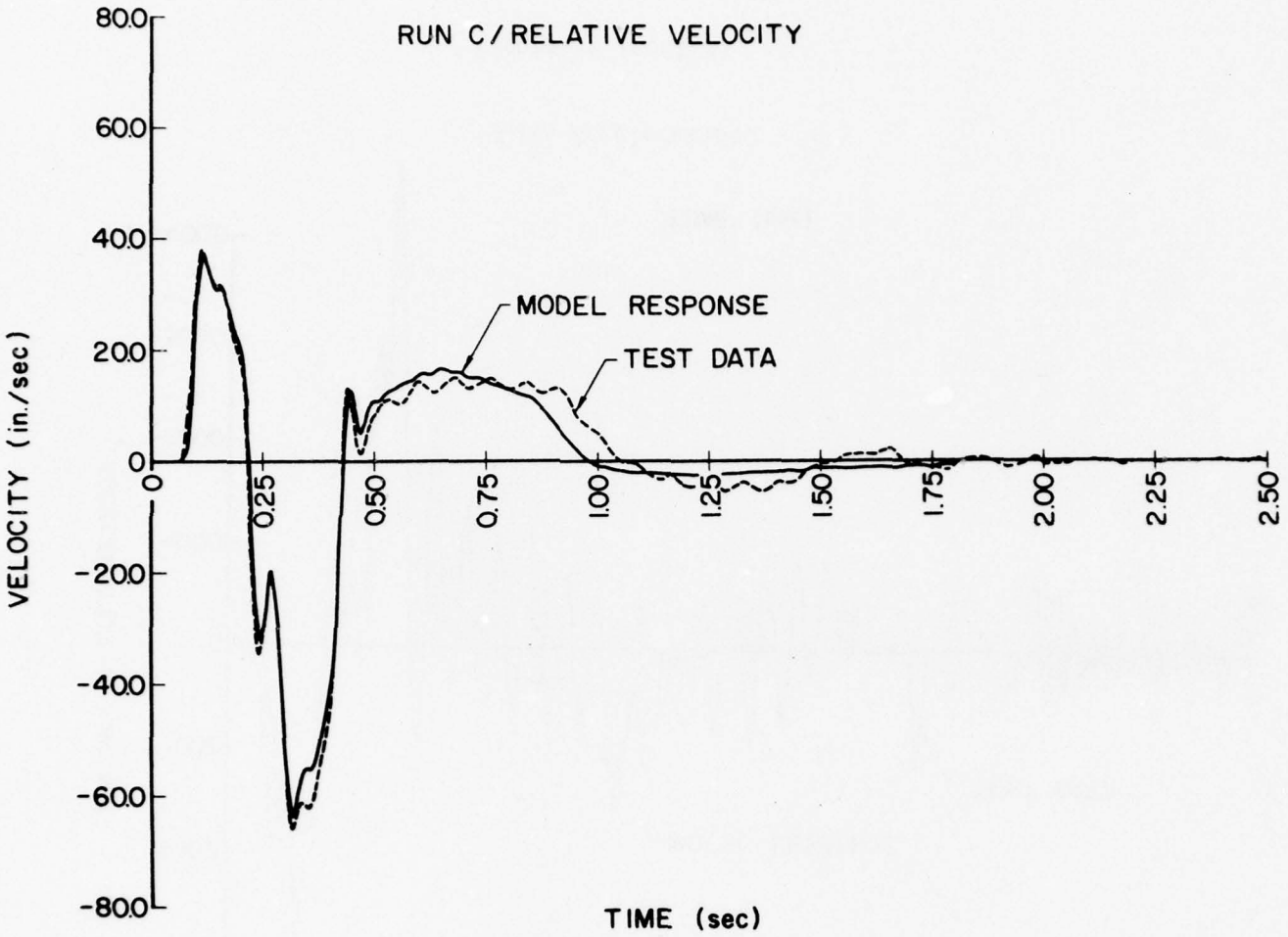

b. Relative Velocity

Figure 16 (cont'd)

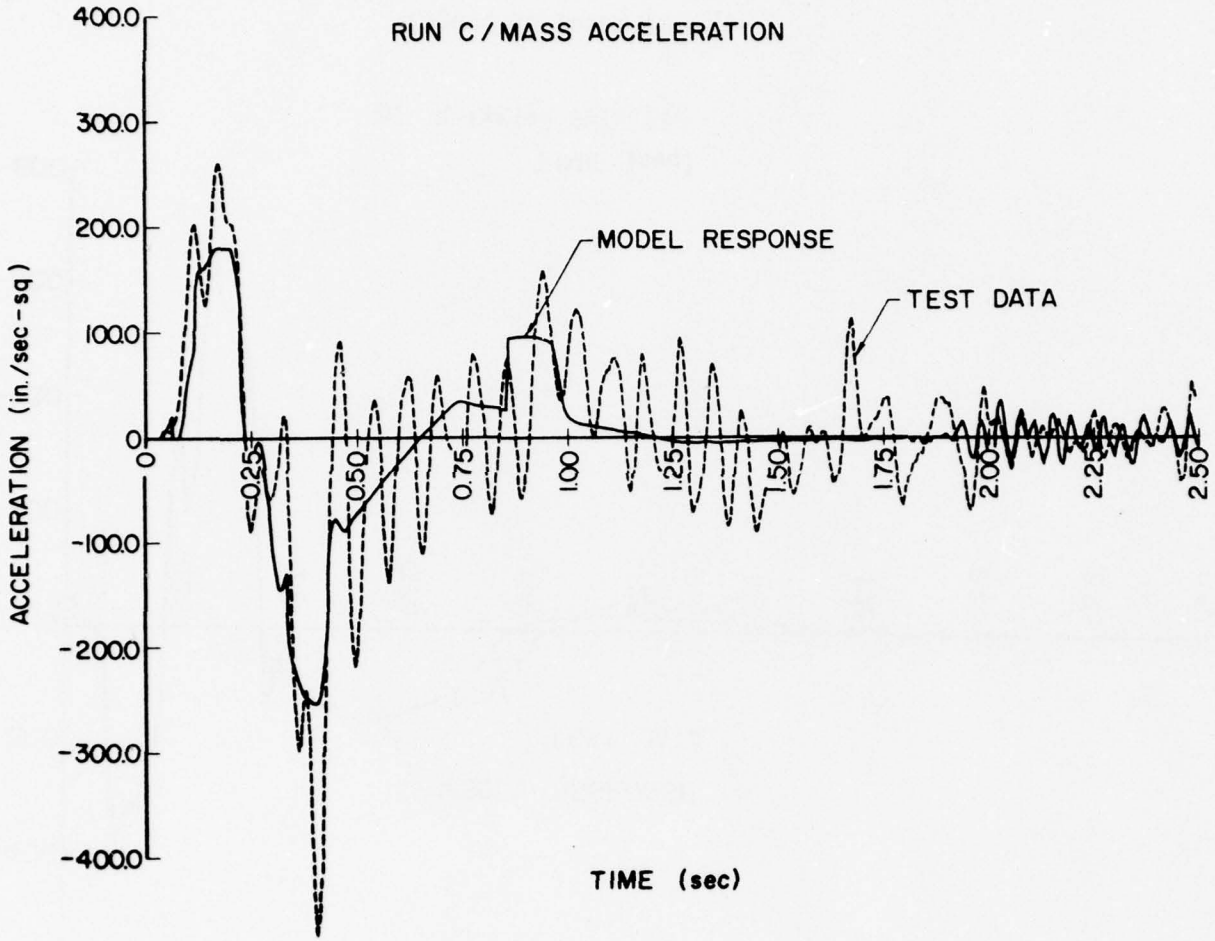

c. Mass Acceleration.

Figure 16 (cont'd)

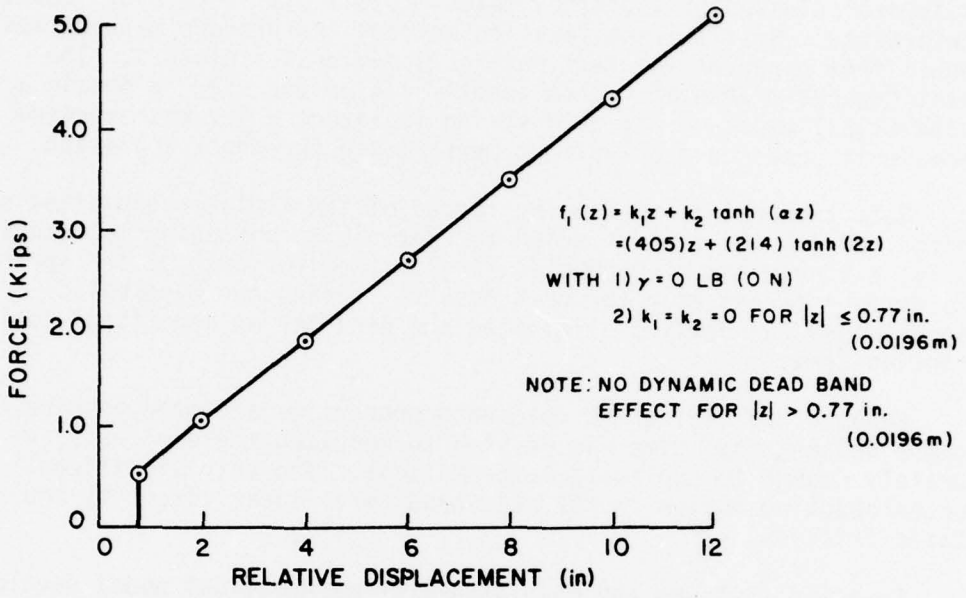

Figure 17. Dynamic spring rate.

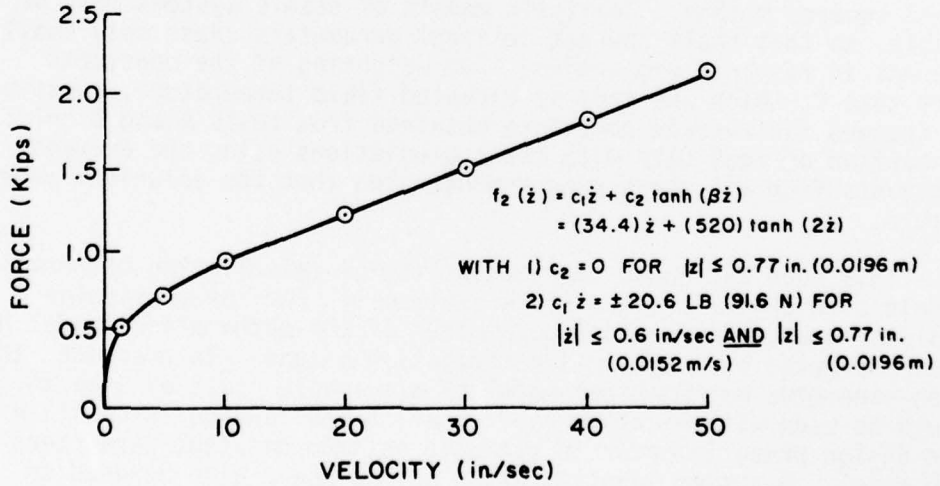

Figure 18. Viscous damping force vs. velocity.

5 CONCLUSIONS

The lack of reasonably accurate open-parameter mathematical models of typical classes of isolators makes it difficult to predict isolator performance. System-identification methods can produce mathematical models from experimental test data on individual isolators. The least-squares method of system identification was used to obtain a mathematical model of a liquid spring isolator, which was selected because it provides near-optimum performance for shock isolation.

Both the spring and damping forces of the isolator exhibited softening. Of all the methods tried for describing softening mathematically, a linear and a hyperbolic tangent term for each of the spring and damping forces gave the best results. Using the hyperbolic tangent term for damping eliminated the need for an additional coulomb friction term.

Because preloading and dead-band properties affected peak response values, some time was devoted to modeling these effects accurately enough to duplicate large motions. The only significant forces opposing motion in the dead band were linear viscosity and static friction.

Equation 10 gives the open parameter mathematical model developed for the isolator. Table 1 gives the optimum values of the parameters for each of the three tests, together with average values.

Comparing model predictions to real data, using optimum constants from test A alone, showed the accuracy that can be achieved by the least squares method. Realistic models of stable systems must be stable, so that small changes in input parameters cause only small changes in response properties. The weighting of the constants from test C, which was made at elevated fluid temperature, substantially changed the average constants obtained from tests A and B only. A comparison of real data with model predictions using the averaged constants from all three runs demonstrated that the solutions were stable.

This work has shown the feasibility of establishing mathematical models of high-performance shock isolators. For the particular isolator used, the constant parameters of the mathematical model have been estimated by a system-identification method. In practice, the open-parameter mathematical model of a suitable class of isolators would be used with platform configuration and loading information in the design phase in order to estimate optimum constant parameters of the model. A system identification method would also be used to estimate the optimum parameters. Knowledge of both the mathematical model and the optimum parameters permits analytical verification of the

isolation system performance before hardware is designed. Spring rate and damping curves can then be specified for optimum performance. The final phase of converting this information into hardware dimensions warrants further research and coordination of results presently found in isolator hardware design literature. This problem has not been addressed in this report.

APPENDIX A:

LEAST-SQUARES SOLUTION FOR
COEFFICIENT PARAMETERS

In Equation 10, the Arabic parameters (k_1, k_2, c_1, and c_2) may be treated as the unknown quantities to be optimized using the least-squares method of system identification. Although other methods might prove more profitable, the least-squares method was basic and could be applied directly.

The constants denoted by lower-case Greek letters (α and β) appear in nonlinear factors that form the known coefficients (from experimental-response data) of the unknown constants to be optimized. The Greek constants modify the nonlinear form of the known values in the matrix of equations to be solved, and therefore they modify the form of the mathematical model. Thus the Greek constants had to be adjusted by trial and error in this work. The Arabic constants are the unknowns to be calculated.

The derivation for optimizing the Arabic constants by the least-squares method begins by rewriting Equation 10 as

$$m\ddot{x}_i + z_{ij}k_j = 0,$$

$$i = 1, 2,...I; \; j = 1, 2,...J \qquad \text{[Eq A1]}$$

where standard summation notation is used. Subscript i denotes the i^{th} time step of the digitized experimental data, while subscript j indicates the term in the equation containing the j^{th} unknown constant. Total time steps I are considered, with J total unknown constants to be optimized. The j^{th} unknown constant is k_j. In any test configuration such as that described in Chapter 2, m denotes the mass to be isolated, and $\ddot{x}_i$ is the acceleration of the mass with respect to coordinates fixed in space (that is, absolute acceleration, as opposed to acceleration relative to the table motion). The values of x_i ($i = 1, 2,...I$) come from measured displacement data that have been differentiated twice, and that therefore contain some experimental noise. The z_{ij} values come from the nonlinear products of relative displacement, z, and relative velocity, $\dot{z}$. They also include the lower-case Greek constants as modifying factors, so to know the z_{ij} values, one must know the Greek constants formed from experimental data.

For simplicity and clarity, let

$$y_i = m\ddot{x}_i \qquad \text{[Eq A2]}$$

and

$$\xi_i = -z_{ij}k_j \qquad \text{[Eq A3]}$$

In the least-squares method, minimizing the squared difference, or error, between y_i and ξ_i overall yields the optimum values of the k_j. Therefore, let

$$2S = \sum_{i=1}^{I} (y_i - \xi_i)^2 \qquad \text{[Eq A4]}$$

where S is a constant. Setting the partial derivative of Eq A4 with respect to each k_j equal to zero minimizes S with respect to each k_j and produces a system of J simultaneous linear algebraic equations of the form

$$\frac{\partial S}{\partial k_j} = \sum_{i=1}^{I} (y_i - \xi_i) \frac{\partial \xi_i}{\partial k_j} = 0 \qquad \text{[Eq A5]}$$

Substituting Equation A3 into Equation A5 gives

$$\sum_{i=1}^{I} (y_i + z_{ij}k_j)(z_{ij}) = 0 \qquad \text{[Eq A6]}$$

For matrix computational purposes, Equation A6 is rewritten as

$$\sum_{i=1}^{I} z_{ji}z_{ij}k_j = -\sum_{i=1}^{I} z_{ji}y_i \qquad \text{[Eq A7]}$$

where z_{ji} is the transpose of z_{ij}. In matrix notation, Equation A7 is

$$[z^T][z]\{k\} = -[z^T]\{y\} \qquad \text{[Eq A8]}$$

where [z] is a J x I rectangular matrix and $[z^T]$ is its transpose. Then {k} is a J x 1 column matrix of the unknown constants, and {y} is an I x 1 column matrix.

Now denoting

$$[A] = [z^T][z] \qquad \text{[Eq A9]}$$

as a J x J matrix of known values from experimental data, and

$$\{b\} = [z^T]\{y\} \qquad \text{[Eq A10]}$$

as a J x 1 column matrix of known values from the data, the final form of the matrix equation to be solved is

$$[A]\{k\} = \{b\} \qquad \text{[Eq A11]}$$

Equation A11 is a well-known problem in matrix algebra. A suitable subroutine for solving Equation A11 for the column of constants $\{k\}$ can be found in programming literature and need not be discussed here. Using such a subroutine, one can find the optimum Arabic constants for a given mathematical model of an isolator.

The overall variance and the covariance matrix are highly useful for analyzing goodness of fit of a model to data. The overall variance, σ^2, is obtained by averaging the mean square error corrected for bias. The error, ε_i, at each time step was used in Equation A4 and may be written in matrix form as

$$\{\varepsilon\} = \{y\} - \{\varepsilon\} \qquad \text{[Eq A12]}$$

where all three terms are I x 1 column matrices. Averaging the squared errors overall i provides a biased estimate of the variance, σ^2:

$$\overline{\sigma}^2 = \frac{1}{I} \langle\varepsilon\rangle \{\varepsilon\} \qquad \text{[Eq A13]}$$

where $\langle\varepsilon\rangle$ is the transpose of $\{\varepsilon\}$, or a 1 x I row matrix. Reducing I by the number of unknown constants, J, to be estimated renders the variance unbiased (σ^2):

$$\sigma^2 = \frac{1}{I - J} \langle\varepsilon\rangle \{\varepsilon\} \qquad \text{[Eq A14]}$$

If N is much larger than J, the biasing influence will be negligible.

The covariance matrix, [V], is J x J and indicates the accuracy and independence of the individual estimators (the unknown constants to be optimized). This matrix is calculated from the relation:

$$[A][V] = \sigma^2[I] \qquad \text{[Eq A15]}$$

where all matrices are J x J, and [I] is unit diagonal. Here [A], σ^2, and [I] are known quantities, and [V] is the unknown matrix to be calculated. [V] can be solved using the same subroutine as used for obtaining {k} in Equation A11.

The numerical value of σ^2 and the conditioning of the [V] matrix were continuously monitored through the trial-and-error process of varying the form of the mathematical model and the lower-case Greek constants. As the model's fit improves, the value of σ^2 decreases, and the principal diagonal elements of [V] grow significantly larger than the off-diagonal elements. These changes indicate good conditioning and imply that the individual terms of the equation are independent.

Accounting for displacements, dead-band, and static-friction effects requires minor condition statements in the computer program. Usually relative motion was assumed (or forced) to be zero whenever $|z| \leq \delta$ and $|\dot{z}| \leq \varepsilon$, but eliminating many of the points where the relative motion was zero produced a better-fitting curve. For example, in Figure 14a, relative motion essentially ceased between 1.50 sec and 2.12 sec. If this portion of the test were included in the least-squares solution, a good fit in this region would be obtained at the expense of less accurate fits of the more significant portions of the curves. Since getting a good fit of the data for no relative motion was trivial, the majority of these points were eliminated.

Preloading was accounted for originally by adding the term $\gamma \mathrm{sgn}(z)$ to Equation 10. In this case, γ was a constant coefficient, so the least-squares analysis ought to optimize it automatically. The relatively small influence of this term in the [A] matrix (for this particular isolator) caused poor conditioning of the corresponding diagonal element in the [V] matrix. Therefore, the value of $\gamma = 0$ was verified by trial and error instead.

APPENDIX B:

TIME DOMAIN SOLUTION OF THE
DIFFERENTIAL EQUATION

Comparison of the analytical and experimental results made it necessary to superimpose the solution of the optimized differential equation on the real data, as done in Chapter 4. Since computer storage and speed of solution were not serious problems, a fourth-order Runge-Kutta algorithm[14] was used to solve the equation. This algorithm was selected for its simplicity and common usage.

In the least-squares solution for the optimized coefficients, the response behavior in the dead-band and static friction had to be accounted for by special programming. Both of these effects occur in regions of small relative displacement and low relative velocity, so they should be of trivial concern for high-performance shock isolation systems. It became apparent, however, that distinct changes in the peak values of the response variables might be directly associated with changes in dead-band and static friction. The solutions remained stable, in that small changes to the dead-band or static friction parameters yielded small changes in peak values of the response variables. Since anything that affects the peak response values should interest designers of isolation systems, the dead-band and static friction modifications were retained as special properties in the Runge-Kutta solution.

In Equation 10, both the linear and hyperbolic tangent terms ($k_1 + k_2 \tanh\alpha z$) for spring forces and the hyperbolic tangent term ($c_2 \tanh\beta\dot{z}$) for damping forces were inactive in the dead band, where $|z| \leq \delta$. Hence linear viscosity ($c\dot{z}$) was the only dynamic force that opposed motion in this band.

Static friction effects were treated differently for initial and terminal motion. Relative motion did not begin until the magnitude of the force applied to the isolator (in this experiment, $F(t) = m\ddot{x}$ was the applied force) exceeded a small static force of $F(t) = 20.6$ lbs (91.6 N). For terminal motion, when $|\dot{u}|$ decreased to zero, the motion of the mass was allowed to continue until $|\dot{z}|$ dropped below $\varepsilon = 0.6$ in./sec (0.0152 m/s). The static friction force in each case was the same, and the average value of $c_1 = 34.4$ from Table 1 was used.

Again, the only reason for considering dead-band and static friction effects was because of their noticeable influence on peak response

[14] B. Carnahan, H. A. Luther, and J. O. Wilkes, *Applied Numerical Methods* (John Wiley and Sons, 1969).

motions. This study made no attempt to model the motion near the rest condition in the dead band with high accuracy. The intent was to model effective conditions for those properties that would yield consistent results and better accuracy for the peak values.

The average constants from Table 1 repeated below reflect the modifications made to the solution programming to account for displacement dead-band, static friction, and preloading effects.

$$k_1 \begin{cases} = 405 \text{ lbs/in.} & \text{for } |z| > \delta \\ = 0 & \text{for } |z| \leq \delta \end{cases}$$

$$k_2 \begin{cases} = 214 \text{ lbs} & \text{for } |z| > \delta \\ = 0 & \text{for } |z| \leq \delta \end{cases}$$

$c_1 = 34.4$ lbs/in./sec for all z and $\dot{z}$

$$c_2 \begin{cases} = 520 \text{ lbs} & \text{for } |z| > \delta \\ = 0 & \text{for } |z| \leq \delta \end{cases}$$

$\gamma = 0.0$ lb (preloading) (0.0 N)

$\delta = 0.77$ in. (0.0196 m) (displacement dead space)

$z = \dot{z} = 0$ for $c_1\dot{z} \leq 20.6$ lb (91.6 N) (initial motion) or $\dot{z} \leq 0.6$ in./sec (0.0152 m/s) (terminal motion) (static friction)

CITED REFERENCES

Carnahan, B., H. A. Luther, and J. O. Wilkes, *Applied Numerical Methods* (John Wiley and Sons, 1969).

CERL Telephone Memorandum from B. Wendler to Taylor Devices, Inc., dated 25 August 1976.

Collins, J. D., et al., "Methods and Applications of System Identification in Shock and Vibration," *System Identification of Vibrating Structures* (American Society of Mechanical Engineers [ASME], 1972).

Courant, R. and D. Hilbert, "Methods of Mathematical Physics," Vol II, *Partial Differential Equations* (John Wiley and Sons, 1962), p 227.

Crandall, S. H. and W. D. Mark, *Random Vibration in Mechanical Systems* (Academic Press, 1963), p 62.

Crawford, R. E., C. J. Higgins, and E. H. Baltman, *A Guide for the Design of Shock Isolation Systems for Ballistic Missile Defense Facilities,* Technical Report S-23 (Construction Engineering Research Laboratory, 1973), p 247.

Cunningham, W. J., *Introduction to Nonlinear Analysis* (McGraw-Hill, 1958), p 76.

Investigation of Optimum Passive Shock Isolation Systems, Technical Report No. AFWL-TR-72-148 (Air Force Weapons Laboratory, 1973), p 154.

Sevin, E., et al., *Computer-Aided Design of Optimum Shock Isolation Systems,* Shock and Vibration Bulletin 39-4 (Naval Research Laboratory, 1969), pp 185-198.

Taylor, D. B., *Application of the Hydraulic Shock Absorber to a Vehicle Crash Protection System,* Society of Automotive Engineers Paper No. 710537 (Society of Automotive Engineers, June 1971), pp 6, 7, 9-11.

Timoshenko, S., D. H. Young, and W. Weaver, *Vibration Problems in Engineering* (John Wiley and Sons, 1974), pp 163, 167.

UNCITED REFERENCES

Brandt, R. J., *Considerations on the Selection of Shock Isolation Systems for the SAFEGUARD Program,* Memorandum No. 6820-1186 (Agbabian-Jacobsen Associates, April 20, 1970).

Crawford, R. E., et al., *The Air Force Manual for Design and Analysis of Hardened Structures*, AFWL-TR-74-102 (Air Force Weapons Laboratory [AFWL], October 1974).

Harris, C. M., and C. E. Crede, *Shock and Vibration Handbook*, 3 Vols (McGraw-Hill, 1961).

Kendall, M. G. and A. Stuart, *The Advanced Theory of Statistics*, 3 Vols (Hafner Publishing Company, 1969).

Mood, A. M. and F. A. Graybill, *Introduction to the Theory of Statistics* (McGraw-Hill, 1963).

Pilkey, W., and B. Pilkey, *Shock and Vibration Computer Programs--Reviews and Summaries* (Naval Research Laboratory, 1975).

Safford, A. A. and R. E. Walker, *Hardness Program Non-EMP In-Place Testing of Shock Isolation Systems for SAFEGUARD TSE Ground Facilities*, R-7317-3757, Contract No. DACA 87-73-0035 (U.S. Army Corps of Engineers, 1975).

Shock Isolation Design Manual, HNDSP-73-98-ED-R (USACE, August 1973).

Study of Shock Isolation for Hardened Structures, AD 639303, Contract No. DA-49-120-ENG-532 (Office of the Chief of Engineers, June 1966).

SYMBOLS

a	Constant
b	Substitution column vector
c	Constants, subscripted, for damping coefficients
d	Differential symbol
f	Nonlinear function, subscripted, for spring and damping effects
i	Summation index for time
j	Summation index for unknown parameters
k	Constants, subscripted, for spring coefficients; also used for general coefficients
m	Mass
n	Summation index for series expansion terms
t	Time
u	Table displacement (absolute)
x	Mass displacement (absolute)
y	Substitution variable
z	Relative displacement
A	Substitution matrix
F	Applied forces
I	Maximum number of digitized time points; also used for unit diagonal matrix
J	Maximum number of unknown parameters
N	Maximum number of series expansion terms
S	Constant
T	Transpose matrix symbol
V	Covariance matrix

SYMBOLS (Cont'd)

Z	Known variable matrix
α, β, γ, δ, ε	Known constants used in nonlinear factors
ξ	Substitution variable
σ	Standard deviation (σ^2 = variance)
$\sum$	Summation symbol
∂	Partial derivative symbol
[]	Rectangular matrix
{}	Column matrix
<>	*Row matrix*

CERL DISTRIBUTION

Chief of Engineers
ATTN: DAEN-RDL
ATTN: DAEN-MCE-D
ATTN: DAEN-ASI-L (2)

USA-WES
ATTN: WEL

US Army Division Engineer
Huntsville
ATTN: Chief, Engr Div

US Army Division Engineer
Missouri River
ATTN: Chief, Engr Div

US Army District Engineer
Omaha
ATTN: Chief, Engr Div

AFWL/DES
Kirtland AFB, NM 87117

Civil Engineer Laboratory
Port Hueneme, CA 93043

Defense Documentation Center (12)

Civil Nuclear Systems Corporation
ATTN: R. E. Crawford
Albuquerque, NM 87102

Sonnenburg, Paul N
Liquid-spring shock isolator modeling / by P. N. Sonnenburg, B. H. Wendler and W. E. Fisher. -- Champaign, Ill. : Construction Engineering Research Laboratory ; Springfield, Va : for sale by National Technical Information Service, 1977.
55 p. : ill. ; 27 cm. -- (Technical report - Construction Engineering Research Laboratory ; M-226)

1. Shock absorbers-mathematical models. I. Wendler Bruce H. II. Fisher, Walter E. III. U.S. Construction Engineering Research Laboratory. IV. Title. V. Series: U.S. Construction Engineering Research Laboratory. Technical report ; M-226.